Journal of Medicinal Chemistry

Article

pubs.acs.org/jmc

Identification of Potent and Selective Cathepsin S Inhibitors Containing Different Central Cyclic Scaffolds

Hans Hilpert,*[,†] Harald Mauser,[†] Roland Humm,[†] Lilli Anselm,[†] Holger Kuehne,[†] Guido Hartmann,[‡] Sabine Gruener,[‡] David W. Banner,[§] Joerg Benz,[§] Bernard Gsell,[§] Andreas Kuglstatter,[§] Martine Stihle,[§] Ralf Thoma,[§] Rubén Alvarez Sanchez,[∥] Hans Iding,[⊥] Beat Wirz,[⊥] and Wolfgang Haap*[,†]

[†]Discovery Chemistry, [‡]Cardiovascular and Metabolic Diseases, [§]Discovery Technologies, [∥]Drug Metabolism and Pharmacokinetics, [⊥]Process Research and Synthesis, Pharma Research and Early Development (pRED), F. Hoffmann-La Roche Ltd., Grenzacherstrasse 124, Basel CH-4070, Switzerland

Supporting Information

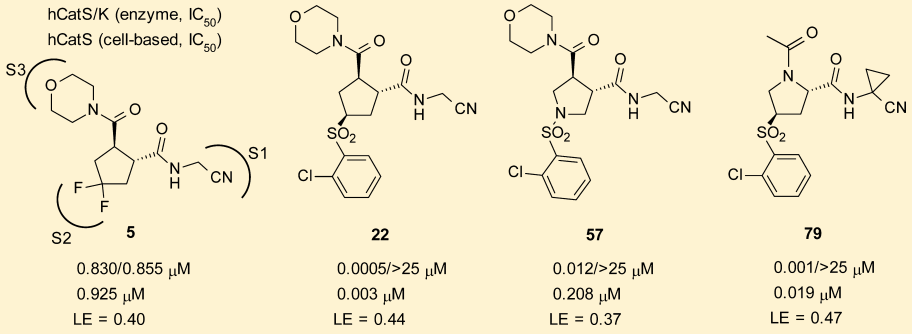

ABSTRACT: Starting from the weakly active dual CatS/K inhibitor **5**, structure-based design supported by X-ray analysis led to the discovery of the potent and selective (>50 000-fold vs CatK) cyclopentane derivative **22** by exploiting specific ligand−receptor interactions in the S2 pocket of CatS. Changing the central cyclopentane scaffold to the analogous pyrrolidine derivative **57** decreased the enzyme as well as the cell-based activity significantly by 24- and 69-fold, respectively. The most promising scaffold identified was the readily accessible proline derivative (e.g., **79**). This compound, with an appealing ligand efficiency (LE) of 0.47, included additional structural modifications binding in the S1 and S3 pockets of CatS, leading to favorable in vitro and in vivo properties. Compound **79** reduced IL-2 production in a transgenic DO10.11 mouse model of antigen presentation in a dose-dependent manner with an ED_{50} of 5 mg/kg.

INTRODUCTION

Cathepsin S (CatS), a lysosomal cysteine protease of the papain family primarily found in B cells, macrophages, and dendritic cells, plays an important role in the antigen-presentation process. Its main function is the degradation of the invariant chain Ii associated with the major histocompatibility complex class II.[1] Gene knockout studies in mice showed defects in immune function, which were also seen with CatS inhibitors,[2,3] but the mice were otherwise healthy and normal in most respects.[4,5] From a variety of preclinical results, there is evidence that CatS inhibition could be beneficial in diseases such as neuropathic pain as well as rheumatoid arthritis, multiple sclerosis, asthma and allergy, chronic obstructive pulmonary diseases, emphysema, Alzheimer's disease, cancer, atherosclerosis, and obesity.[6] CatS as a target has attracted much attention in the pharmaceutical industry because of its pleiotropic nature; therefore, strong efforts have been made to identify potent and selective CatS inhibitors. Selectivity over other cathepsins is of high importance to evaluate the pharmacology of CatS inhibitors and to assess their therapeutic potential in the clinic.

Many of the recent CatS inhibitors contain an electrophilic motif (e.g., a nitrile), which binds covalently and reversibly to cysteine C25 (vide infra) in the active site, forming a thioimidate.[6] This binding motif has been employed, for example, in the aminocyclopropane nitrile **A** by Merck Frosst[7] or in the succinamide derivative **B**[8] and more recent triazoles[9] both described by Boehringer Ingelheim. Cyclohexyl-substituted derivatives (e.g., **C**) were developed as CatK inhibitors at Roche more than a decade ago[10] and served as a basis for the development of selective CatS inhibitors. Compound **C** is a selective CatK inhibitor with modest activity at CatS (CatS/K, IC_{50} = 0.640/0.016 μM). To change the selectivity in favor of CatS, 1,2,4-substituted five-membered scaffolds **D** (Figure 1) with three residues attached to the scaffold orientated toward the S1−S3 pockets of the CatS active site were investigated (supported by molecular modeling). Selectivity for CatS could be accomplished by an appropriate extended R^2 residue pointing

Received: October 1, 2013

   dx.doi.org/10.1021/jm401528k | J. Med. Chem. XXXX, XXX, XXX−XXX

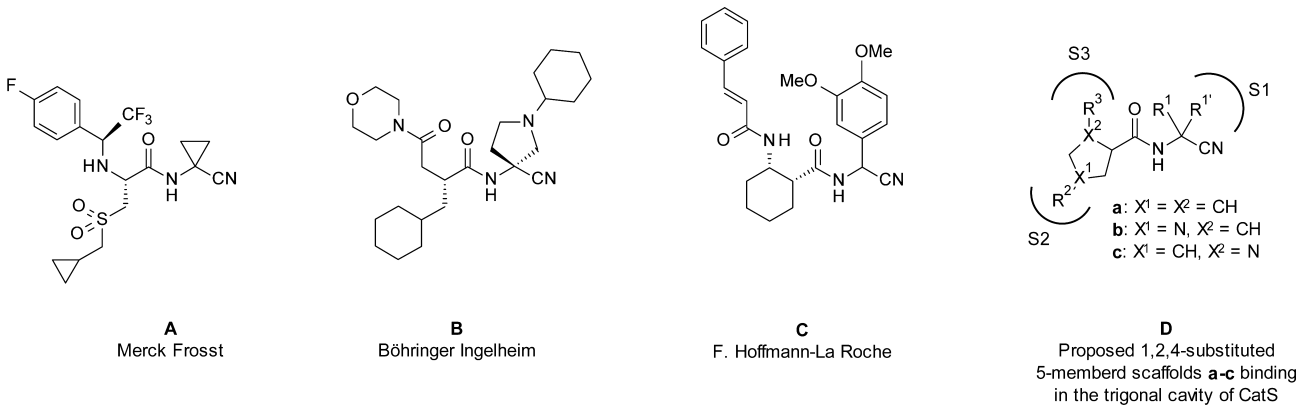

Figure 1. Known CatS inhibitors **A**–**C** and design of new inhibitors **D**.

Scheme 1. Synthesis of R^1- and R^2-Modified Cyclopentane Derivatives 5 and 20–26[a]

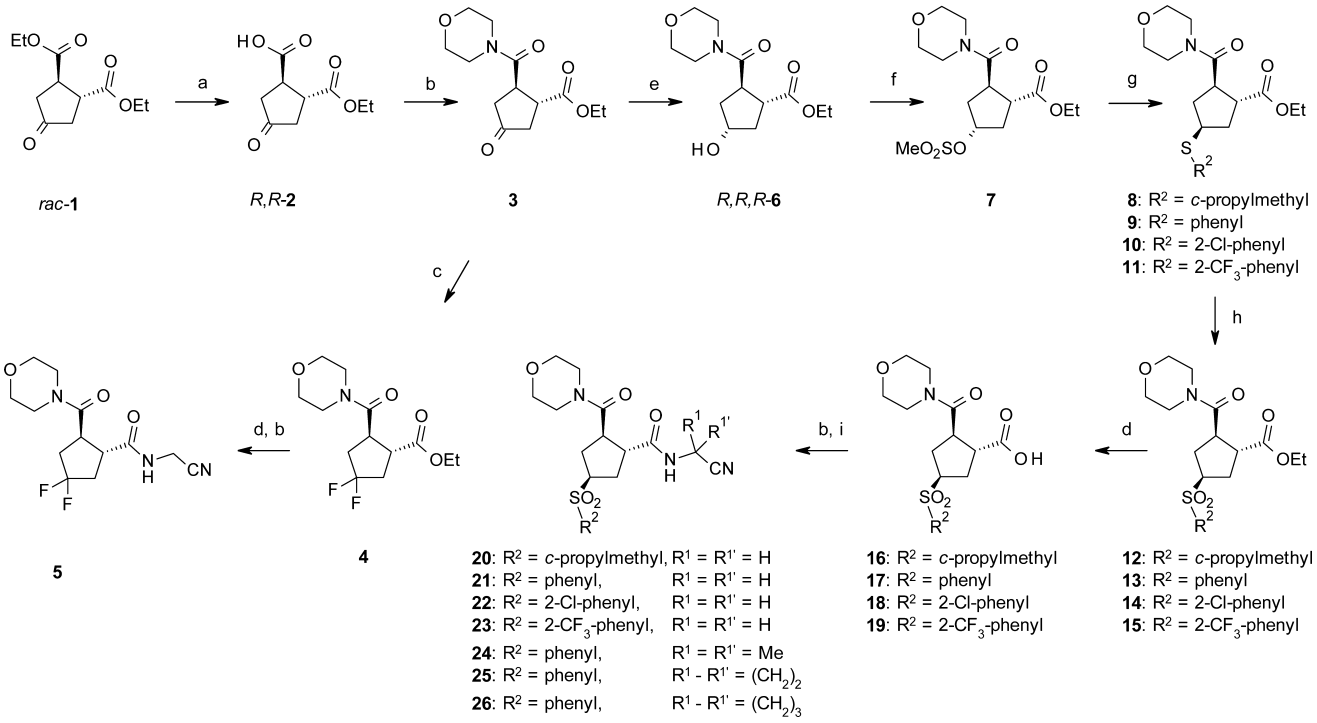

[a]Reagents and conditions: (a) CALB L (lipase from *Candida antarctica* B, Novozymes), aqueous buffer (pH 6.2), 22 °C. (b) **3**; morpholine, **5** and **20**–**23**; aminoacetonitrile hydrochloride, EDCI, HOBt, THF, Et_3N, 22 °C. (c) DAST, CH_2Cl_2, 5 to 22 °C. (d) LiOH, MeOH, THF, H_2O, 22 °C. (e) NADP, glucose dehydrogenase GDH 102 (Codexis), ketoreductase KRED-NADP-131(Codexis), aqueous buffer (pH 6.5), 22 °C. (f) MsCl, Et_3N, CH_2Cl_2, 5 °C. (g) **8**; cyclopropylmethylthiol, **9**; thiophenole, **10**; 2-chlorothiophenol, **11**; 2-trifluoromethylthiophenol, NaH, THF, 50 °C. (h) *m*-Chloroperbenzoic acid, CH_2Cl_2, 22 °C. (i) **24**; 2-Amino-2-methyl-propionitrile hydrochloride, **25**; 1-amino-cyclopropanecarbonitrile hydrochloride, **26**; 1-aminocyclobutane-1-carbonitrile, *i*-butyl chloroformate, 4-methyl-morpholine, THF, −16 to 22 °C.

into the S2 pocket of CatS, which is significantly smaller in CatK (vide infra).

The rigidity of a cyclic scaffold can be of advantage to reduce the number of rotatable bonds, thereby making the inhibitors less prone for metabolic break down and more potent if the appropriate binding conformation is populated. We explored five-membered rings **D** such as cyclopentanes **a**, pyrrolidines **b**, and prolines **c** as homo- and heterocyclic scaffolds. Scaffolds **a**[11] and **c**[12] were already disclosed in patents three years ago, and more recently Kim et al.[13] and F. Hoffmann-La Roche[14] described proline scaffold **c** as well with a keto-heterocycle attached to it, which binds in the S1 pocket.

CHEMISTRY

The syntheses of cyclopentane derivatives **5** and **20**–**26**[11] having modifications at R^1 and R^2 start with the racemic trans ester **1** (Scheme 1), which is readily prepared from commercial 3,4-dicarboxy-hexanedioic acid on a multigram scale.[15] An efficient enzymatic hydrolysis of *rac*-**1** gave access to chiral acid **2** as the formed *R,R*-enantiomer (ee 95%), requiring the highly selective lipase from *Candida antarctica* B. The screening of a large enzyme library (>100 tested), substrate engineering (Me-, Et-, *n*-Bu-diester), and a quite in-depth process optimization afforded this highly enantioselective and robust enzymatic resolution of *rac*-**1**. Chiral acid **2** was coupled with morpholine using EDCI and HOBt to give amide **3**, which was subjected to diethylamino-

dx.doi.org/10.1021/jm401528k | J. Med. Chem. XXXX, XXX, XXX–XXX

Scheme 2. Synthesis of R^3-Modified Cyclopentane Derivatives 33−46[a]

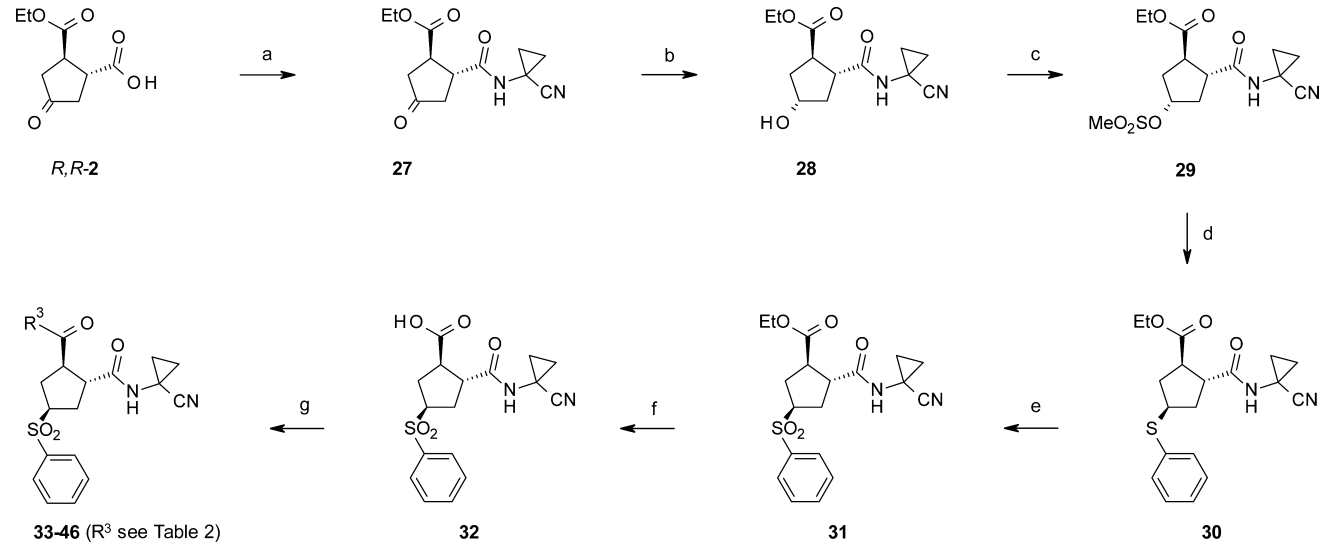

[a]Reagents and conditions: (a) 1-amino-cyclopropanecarbonitrile hydrochloride, *i*-butyl chloroformate, 4-methyl-morpholine, THF, −16 to 22 °C. (b) $NaBH_4$, THF, −15 to 0 °C, inseparable mixture of **28** and its epimer (structure not shown) was obtained. (c) MsCl, Et_3N, CH_2Cl_2, 5 °C, inseparable mixture of **29** and its epimer (structure not shown) was obtained. (d) Thiophenole, NaH, THF, 50 °C. (e) *m*-Chloroperbenzoic acid, CH_2Cl_2, 22 °C. (f) LiOH, MeOH, THF, H_2O, 22 °C. (g) For amines, see Table 2, EDCI, HOBt, THF, Et_3N, 22 °C.

Scheme 3. Synthesis of R^2-Modified Pyrrolidines 56−58[a]

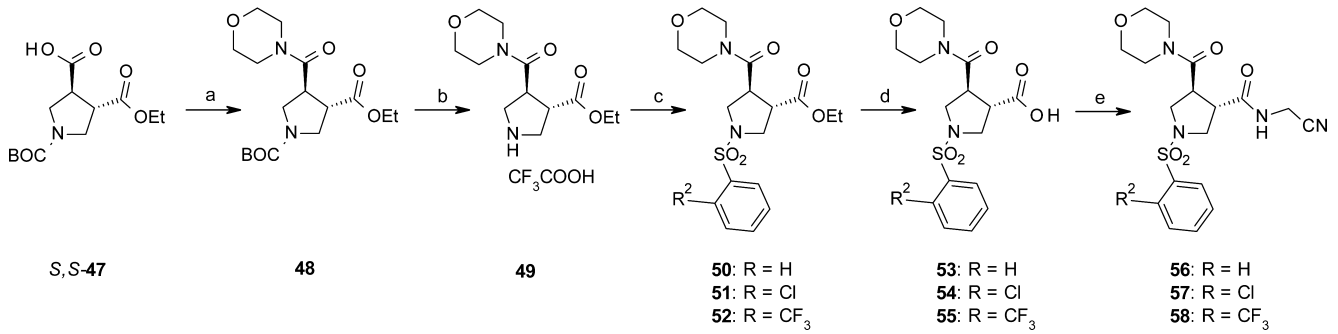

[a]Reagents and conditions: (a) morpholine, EDCI, HOBt, THF, 22 °C. (b) Trifluoroacetic acid, CH_2Cl_2, 22 °C. (c) **50**; phenylsulfonyl chloride, **51**; 2-chlorophenylsulfonyl chloride, **52**; 2-trifluoromethylphenylsulfonyl chloride, $(i\text{-Pr})_2EtN$, THF, 22 °C. (d) LiOH, MeOH, THF, H_2O, 22 °C. (e) Aminoacetonitrile hydrochloride, EDCI, HOBt, Et_3N, CH_3CN or DMF, 22 °C.

sulfur trifluoride (DAST), furnishing difluorocylopentane derivative **4**. Hydrolysis of the ester group in **4** to the acid (structure not shown) using LiOH followed by coupling with aminoacetonitrile using EDCI/HOBt delivered desired target compound **5**. The reduction of ketone **3** to the required R,R,R-configured alcohol **6** with $NaBH_4$ was difficult to achieve, yielding a 1:2 mixture of **6** and its undesired epimer (structure not shown), which were inseparable by chromatography on silica. It appears that the attack of the hydride occurred preferentially from the sterically less hindered site (i.e., opposite of the larger morpholino substituent in **3**), furnishing the undesired epimer preferentially.

A powerful method to change the course of selectivity was found by an enzymatic reduction of **3** using ketoreductase KRED-NADP-131 and the most widely applied cofactor-recycling system based on D-glucose as final reductant and glucose dehydrogenase.[16,17] This ketoreductase was the single highly selective screening hit out of >100 enzymes tested, providing *R,R,R*-alcohol **6** with a high de of 95%. The subsequent activation to mesylate **7** enabled the substitution by thioalcohols, furnishing thioethers **8**−**11** with inversion of the configuration. Oxidation of the thioethers to sulfones **12**−**15** was accomplished with *m*-chloroperbenzoic acid, and the ester group was then hydrolyzed to acids **16**−**19**. Targeted amides **20**−**23** were prepared using EDCI/HOBt as the coupling reagents, whereas access to the sterically more demanding substituted amino-acetonitriles **24**−**26** required the activation via a mixed anhydride using *i*-butyl chloroformate. The relative and absolute configurations of **20**−**26** were assigned on the basis of an X-ray structure of **21** bound to mouse CatS.

To evaluate variations in the S3 binding pocket, the sequence of reactions was changed (Scheme 2). Acid *R,R*-**2** was first converted to amido-cyclopropanecarbonitrile **27** followed by reduction of the keto group to alcohol **28** using $NaBH_4$. The selectivity was again driven by the sterically more demanding amido-cyclopropanecarbonitrile residue, affording this time a 2:1 mixture in favor of desired alcohol **28** and its epimer (structure not shown), which were again inseparable by chromatography. Thus, the epimer-mixture was converted via mesylate **29** to thioether **30**, at which stage the separation of the epimers was

dx.doi.org/10.1021/jm401528k | J. Med. Chem. XXXX, XXX, XXX−XXX

Scheme 4. Synthesis of R^2- and R^3-Modified Prolines 76−79[a]

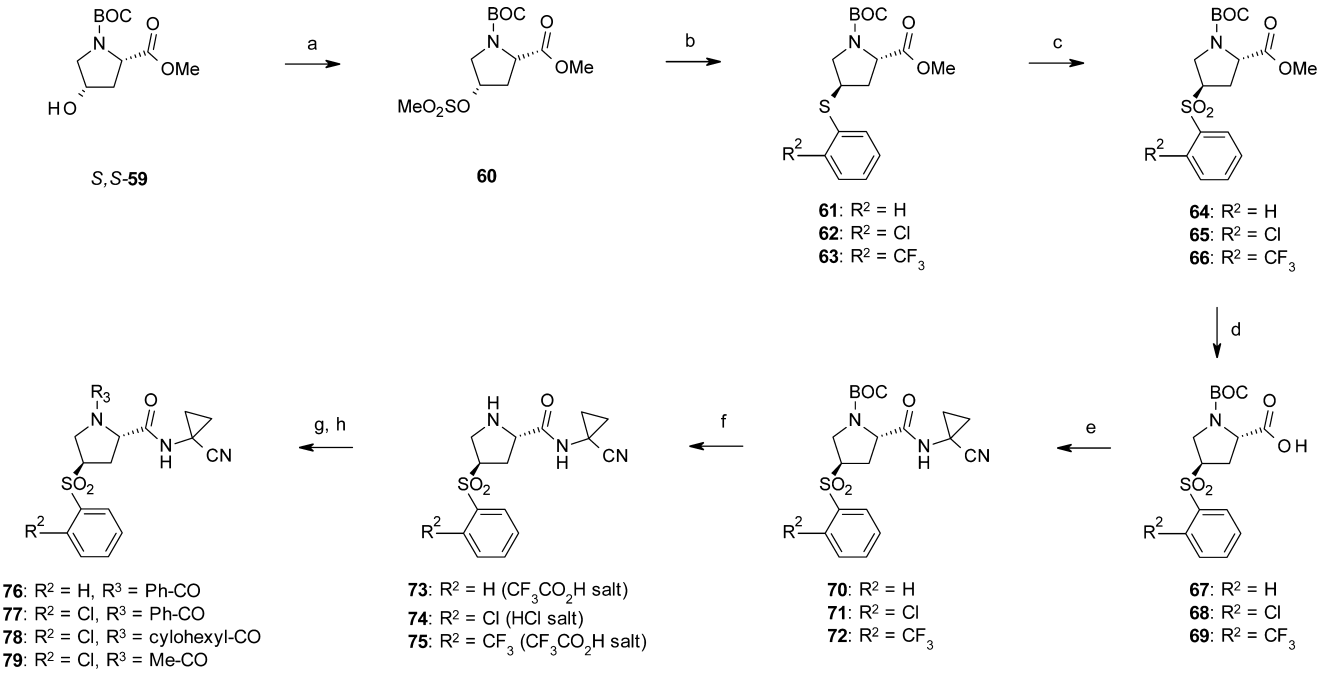

[a]Reagents and conditions: (a) MsCl, Et_3N, CH_2Cl_2, 5 °C. (b) **61**; thiophenol, **62**; 2-chlorothiophenol, **63**; 2-trifluoromethylthiophenol, NaH, THF, 50 °C. (c) *m*-Chloroperbenzoic acid, CH_2Cl_2, 22 °C. (d) LiOH, MeOH, THF, H_2O, 22 °C. (e) 1-Amino-cyclopropanecarbonitril hydrochloride, *i*-butyl chloroformate, 4-methyl-morpholine, THF, −16 to 22 °C. (f) Trifluoroacetic acid/CH_2Cl_2 or HCl/1,4-dioxane, 22 °C. (g) **76** and **77**; benzoic acid, **78**; cyclohexanecarboxylic acid, EDCI, HOBt, THF or DMF, Et_3N, 22 °C. (h) **79**; acetic anhydride, CH_3CN, $(i\text{-Pr})_2EtN$, 22 °C.

possible. Oxidation of **30** to **31** and hydrolysis yielded targeted acid **32**, which served as the starting material for a series of compounds, **33**−**46**,[11] having R^3 modified (Table 2). To confirm the relative and absolute configurations of **33**−**46**, acid **32** was reacted with morpholine to give compound **25**, which was identical, according to ^1H NMR, with **25** prepared according to Scheme 1.

The synthesis of pyrrolidines **56**−**58** (Scheme 3) starts from known chiral acid *S,S*-**47**, which is readily accessible on a multigram scale in three steps.[18] Amide formation and deprotection of the BOC group yielded pyrrolidine **49**, which was converted to sulfonamides **50**−**52**. Hydrolysis of the ethyl ester and amide formation completed the synthesis of **56**−**58** in the same manner as outlined in Scheme 1.

Finally, prolines **76**−**79**[12] (Scheme 4) were made available starting with commercially available homochiral hydroxy-proline derivative *S,S*-**59**. Formation of mesylate **60** followed by substitution with thiophenols and oxidation yielded sulfones **64**−**66** in an analogous manner to that previously discussed. Hydrolysis of the methyl ester in **64**−**66** followed by amide formation and deprotection of the BOC group furnished proline derivatives **73**−**75**, which served as the key intermediates for the introduction of R^3 residues, affording final prolines **76**−**79**. The relative and absolute configurations of **76**−**79** were assigned on the basis of an X-ray structure of **75** bound to mCatS (structure not shown, PDB accession number 4BS5).

RESULTS AND DISCUSSION

We started the SAR exploration with the cyclopentane scaffold that was devoid of an R^2 substituent binding in the S2 pocket of CatS. Because the S1 and S3 pockets are largely similar in CatS and CatK, compound **5** turned out to be an unselective dual CatS/K inhibitor with modest activities (IC_{50} = 0.85 μM at both enzymes, Table 1). Extending into the S2 pocket with, for example, the cyclopropylmethyl sulfone residue in **20** resulted in an approximately 4-fold higher enzymatic inhibition of CatS but, more importantly, had a profound effect on CatK selectivity, which improved >100-fold. A number of other alkylsulfones explored were less active (results not shown). Gratifyingly, phenylsulfone **21** boosted the IC_{50} value into the subnanomolar

Table 1. SAR of R^2 Modifications on Cyclopentane Derivatives 5 and 20−23 and Pyrrolidines 56−58

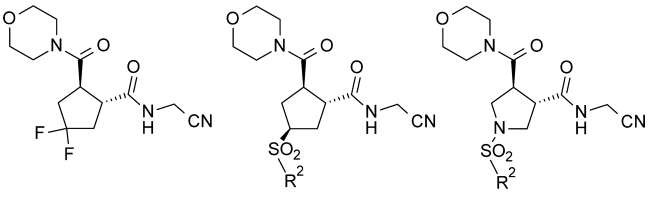

5 **20-23** **56-58**

compd	R^2	IC_{50} (μM)[a] hCatS enzyme	IC_{50} (μM)[a] hCatK enzyme	selectivity hCatK/hCatS	IC_{50} (μM)[a] A20 cell-based[b]
5		0.830	0.855	1	0.925
20	CH_2c-Pr	0.230	>25	>100	4.506
21	Ph	0.0007	15.5	>20 000	0.023
22	2-Cl-Ph	0.0005	>25	>20 000	0.003
23	2-CF_3-Ph	0.0009	>25	>20 000	0.002
56	Ph	0.271	>25	>90	4.239
57	2-Cl-Ph	0.012	>25	>1000	0.208
58	2-CF_3-Ph	0.018	>25	>1000	0.118

[a]IC_{50} values are the mean of at least two independent experiments. The errors of the IC_{50} values are within a factor of 1.6. [b]A20/DO10.11 antigen-presentation assay.

dx.doi.org/10.1021/jm401528k | J. Med. Chem. XXXX, XXX, XXX−XXX

range (IC_{50} = 0.0007 μM) with the desired high selectivity of >20 000-fold versus CatK and showed a high activity of IC_{50} = 0.023 μM in the cellular mouse A20/DO10.11 assay, an assay of ovalbumin-specific antigen presentation. A variety of mono- and disubstituted phenyl residues were explored as well, with all showing uniformly low IC_{50} values in the enzymatic assay, the most notable of which were the 2-Cl- and 2-CF_3-substituted phenylsulfones **22** and **23**, providing an additional 8- and 12-fold increase in cellular activity, respectively, compared to unsubstituted **21**.

Pyrrolidines **56**−**58** with optimized R^2 phenylsulfone residues were investigated as well but turned out to be significantly less active in the enzyme (20−390-fold) as well as cell-based assay (60−180-fold) compared to cyclopentane counterparts **21**−**23**. Interestingly, cellular activity increased again from **56**−**58**, as seen in the cyclopentane series (Table 1).

X-ray Structures of Cathepsin S Inhibitors. Human[19] and mouse CatS have almost identical amino acid sequences and topologies (Figure 2) within the active sites in which our

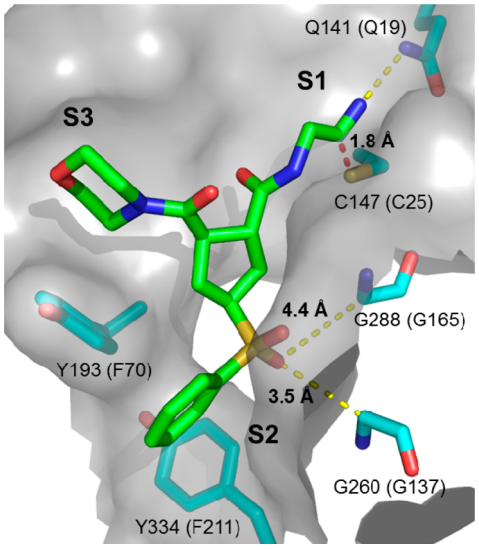

Figure 2. X-ray structure of **21** (green) bound to mCatS (light blue) at 1.96 Å resolution (PDB code 4BSQ). The corresponding amino acids of hCatS are given in parentheses. The nitrile reacts with the catalytic cysteine 147 to form a thioimidate. Glycines 288 and 260 orient the phenyl residue of the inhibitor into the S2 pocket in which favorable edge-to-face interactions with tyrosines 334 and 193 are possible. Figures 2−4 were prepared with the PyMol program.[21]

inhibitors bind. Consequently, IC_{50}'s are similar for both enzymes (vide infra). Because mouse was the in vivo species, both mouse and human CatS were cloned, expressed, purified, and crystallized. In initial parallel trials, it was found that mCatS often crystallized more readily than hCatS, so hCatS was only used for crystallization when mCatS failed.

A first glance, Figure 2 shows the nice fit of a five-membered cyclic scaffold with the three attached residues pointing into the trigonal cavity (S1−S3) of mCatS, as predicted by molecular modeling. Catalytic cysteine 147 (hCatS = C25) forms the central anchoring motif in the S1 binding pocket, which can interact with a variety of known electrophiles.[20] A prominent electrophile is the nitrile group, which undergoes a reversible covalent binding in **21** with a short distance of 1.8 Å, forming a thioimidate anion that is stabilized by a hydrogen bond to Q141. There is space within the cavity of the S1 pocket, suggesting that the R^1 substituents adjacent to the nitrile moiety should be explored (vide infra).

The rather hydrophobic S2 pocket is accessible via a small channel 'gated' by the adjacent glycines 288 and 260. In CatK,[22] these glycines are replaced by more bulky alanines, thus blocking access to the S2 pocket. The sulfone linker in **21** is favorably located in the channel within close van der Waals (vdW) distances to the glycines 288 and 260 (4.4 and 3.5 Å, respectively), positioning the terminal phenyl residue of **21** in a double orthogonal fashion to tyrosines 334 and 193. As a result, a network of four favorable edge-to-face interactions of the three aromatic units (3.1−3.8 Å) contributes to the high activity of IC_{50} = 0.0007 μM. The rather shallow and hydrophilic S3 pocket should tolerate many residues and was therefore explored extensively.

A possible explanation for the reduced enzymatic binding affinity of pyrrolidine **56** versus cyclopentane scaffold **21** (IC_{50} = 0.271 and 0.0007 μM, respectively) can be derived from their X-ray structures bound to mCatS. Both compounds bind in the same conformation (Figure 3a) in the active site of mCatS.

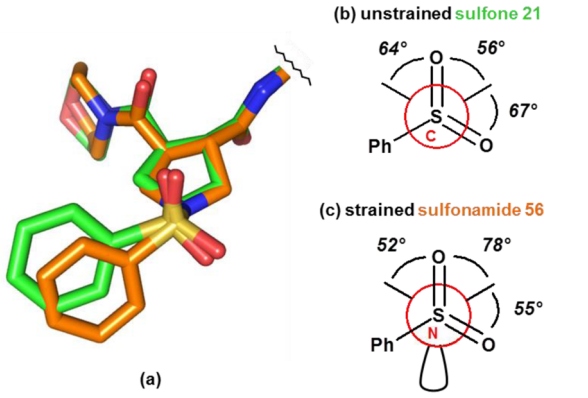

Figure 3. (a) X-ray structures of **21** (green, 1.96 Å, PDB code 4BSQ) and **56** (orange, 1.47 Å, PDB code 4MZO) in the bound conformation with mCatS (not shown). (b) Cyclopentane-sulfone scaffold **21** adopts a low-energy conformation without significant deviation of the dihedral angles from 60°. (c) Pyrrolidine-sulfonamide **56**, however, was found in a high-energy conformation with dihedral angles deviating significantly from 60°, resulting in a 390-fold decreased binding affinity compared to unstrained **21**.

Cyclopentane-sulfone **21** is found in one of the two low-energy conformations without significant deviation of the dihedral angles from 60° (Figure 3b). In contrast to **21**, pyrrolidine-sulfonamide **56** adopts a strained conformation in which the nitrogen lone pair is located in proximity to one of the S═O groups (Figure 3c). Sulfonamides are known to have conformational preferences in which the nitrogen lone pair bisects the O═S═O angle in the Newman projection.[23] It has been suggested that this rotamer is stabilized by the lone pair interaction with the sulfur d orbital.[24] Pyrrolidine-sulfonamide **56**, however, cannot be accommodated in this low-energy conformation in the active site of CatS but was found in a strained conformation with dihedral angles deviating significantly from 60°. This energy consideration is supported by the torsion angles of alkyl-sulfones versus alkyl-sulfonamides observed in the Cambridge Structural Database (CSD).[25,26] The torsion of cyclopentane-sulfone **21** is close to the median of 55°; pyrrolidine-sulfonamide **56** torsion is only found in rare cases, the majority of alkyl-sulfonamides show a torsion of 180° (see Figure 6, Supporting Information). As a

dx.doi.org/10.1021/jm401528k | J. Med. Chem. XXXX, XXX, XXX−XXX

consequence, this strain energy is only partially compensated by the favorable edge-to-face interaction of the aromatic units, which resulted in reduced enzymatic and cell-based activities by more than 2 orders of magnitude.

Another remarkable effect is the approximately 20-fold increased activity in the enzyme and cell-based assay of pyrrolidine **57** substituted with a 2-Cl-phenyl residue compared to unsubstituted phenyl derivative **56** (cf. Table 1). The X-ray structure of **57** complexed with mCatS (Figure 4) shows the

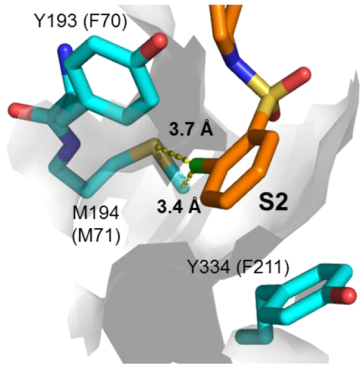

Figure 4. X-ray structure of 2-Cl-phenyl pyrrolidine **57** (orange, 1.85 Å resolution, PDB code 4MZS) bound to mCatS (light blue) in the S2 pocket. The corresponding amino acids of hCatS are given in parentheses. The chlorine atom undergoes a favorable halogen bonding with the methionine sulfur atom (M194) with a short distance of 3.7 Å and a close to ideal S···Cl−C angle of 170°, thereby enhancing binding affinity. In addition, the chlorine atom is in a short distance to the terminal methyl group of M194 (distance epsilon C···Cl, 3.4 Å), indicating a favorable vdW interaction.

same edge-to-face interaction of Y193 with the 2-Cl-phenyl residue (3.6 and 3.9 Å) as seen in **21** (cf. Figure 2). Contrary to **21**, flexible Y334 is no longer undergoing an edge-to-face interaction, instead it undergoes a face-to-face interaction with the more bulky 2-Cl-phenyl residue (3.5 and 3.9 Å) as a consequence of the ortho substituent now occupying the original position of Y334 seen in **21**. Boeckler et al. have predicted the existence of a favorable halogen bonding between the sulfur atom of a methionine residue and a chlorine atom on the basis of quantum mechanical calculations.[27] Indeed, there is a remarkably short distance between the chlorine and the sulfur atom of methionine 194 of 3.7 Å (i.e., close to the sum of the vdW radii of the two interacting atoms, 3.6 Å). In addition, the S···Cl−C angle was found to be 170°, almost representing the ideal angle of 180° required for optimal interactions of a polarizable atom with the sigma hole of the Cl atom as found in halogen bonding.[27,28] The chlorine atom is also making a favorable vdW interaction with the hydrogen atoms of the C-epsilon atom of M194, with the Cl···C-epsilon distance of 3.4 Å being even shorter than the Cl···S distance. 2-CF_3-phenyl-substituted pyrrolidine **58** shows a similar effect (i.e., a 15- and 36-fold increase in enzyme and cell-based activity, respectively, compared to **56**). In summary, shape complementarity, favorable electrostatics, and the movement of Y334 yielding a face-to-face interaction account for this improved potency over the nonsubstituted phenyl derivatives. In the cyclopentane series, **21**−**23**, this effect was not evident in the enzyme (the IC_{50} = 0.0005−0.0009 μM are virtually identical), but it was clearly visible in the cell-based assay (8- and 12-fold increased activity of **22** and **23**, respectively, compared to **21**). The absence of the effect in the enzyme assay can be explained by the assay limitations: compound concentrations lower than 0.001 μM are below the enzyme concentration used in the assay, leading to nonlinear Michaelis−Menten kinetics at low concentrations.

SAR Exploration of Cylopentane and Proline Scaffolds. Cyclopentane derivative **21** served as a basis for a limited number of symmetrical $R^{1,1'}$ variations in the S1 pocket. From three of the compounds evaluated (**24**−**26**, Table 2), cyclopropyl derivative **25** showed a 2-fold increased cell-based activity compared to **21** and was therefore selected for R^3 modifications. Ring-size variations of various heterocycles is well-tolerated (Table 2); six-membered derivatives such as dimethyl-morpholine **33** and piperidines **36** and **37** even showed single-digit nanomolar activity in the cell-based assay. Interestingly, even small dimethyl-amide **46** retained substantial activity in the enzyme as well as cell-based assay (IC_{50} = 0.006 and 0.091 μM, respectively). Terminal polar groups such as a NH or OH (in **39**, **40**, and **45**) or a sulfone (in **41**) impaired the cell-based activity remarkably (IC_{50} = 0.37 − 1.34 μM). This is presumably due to their reduced permeability (e.g., P_{eff}[29] = 0.2/0.2 × 10^{-6} cm/s for **40**/**41** compared to P_{eff} = 4.6 × 10^{-6} cm/s for **37**, as determined in the parallel artificial-membrane-permeability assay (PAMPA)). There seems to be ample scope for R^3 modifications in the S3 binding pocket, as was expected from its shallow nature (vide supra); none of them compromised CatK selectivity (**33**−**46**, IC_{50} > 25 μM).

Keeping the conformation of the sulfone moiety and reducing the chemical complexity of the cyclopentane series, we next explored the proline scaffold. Five examples were evaluated (**75**−**79**, Table 3) that incorporated the optimal cyclopropyl residue $R^{1,1'}$, 2-Cl- and 2-CF_3-phenyl sulfones as R^2, and a few simple R^3 residues (Ph, cyclohexyl, Me, and H). Gratifyingly, most of the compounds showed high activity in the enzyme and cell-based assays, with cyclohexyl derivative **78** being the most potent. Again, *o*-Cl-phenylsulfone **77** was approximately 15-fold more potent in the enzyme and cell-based assays compared to unsubstituted phenylsulfone **76**. In preparation for in vivo studies in mice, selected examples were also tested against mouse CatS. As expected, cyclopentane **21** and prolines **75**−**79** showed similar activities in h- and mCatS (Table 3) on the basis of their almost identical amino acid sequences and topologies in the active site (cf. Figure 2). Furthermore, the compounds were, in general, highly selective over CatK, L, and B (cf. Tables 2 and 3).

In Vivo Pharmacokinetics (PK) and Pharmacodynamics (PD) of CatS Inhibitors. With the aim of studying being the pharmacokinetics and pharmacodynamics of the CatS inhibitors, the compounds shown in Table 3 were tested in vitro for enzymatic proteolytic degradation in human and mouse plasma. Compounds **77** and **78** were unstable in mouse (>90% degraded after 4 h), whereas **21**, **75**, and **79** turned out to be sufficiently stable in mouse (99, 51, and 72% remaining after 4 h, respectively) and were fully stable in human plasma 5 h after incubation, rendering them suitable for in vivo PK characterization. When tested in mouse PK studies, cyclopentane derivative **21** exhibited a medium systemic clearance and a moderate oral bioavailability, resulting in modest exposure levels upon oral administration (Table 4). In contrast, prolines **75** and **79** showed more suitable PK properties on the basis of their better bioavailability and higher AUC after po administration and were thus further profiled for in vivo pharmacology studies.

Transgenic DO10.11 mice (expressing an ovalbumin-specific T-cell receptor) were challenged to ovalbumin once. The compound was given 30 min before ovalbumin challenge by oral

dx.doi.org/10.1021/jm401528k | J. Med. Chem. XXXX, XXX, XXX−XXX

Table 2. SAR of R^1 and R^3 Modifications on Cylopentane Derivatives 21, 24−26, and 33−46

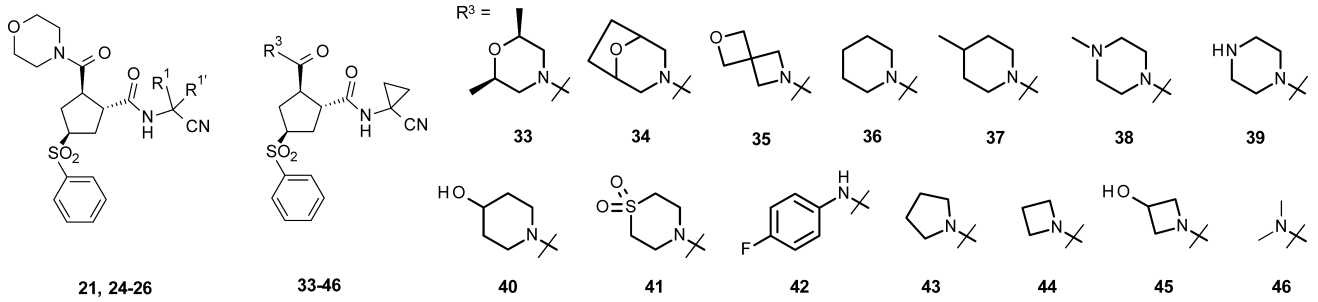

			IC_{50} (μM)[a]				
compd	R^1	$R^{1'}$	hCatS enzyme	hCatK enzyme	hCatL enzyme	hCatB enzyme	A20 cell-based[b]
21	H	H	0.0007	15.5	11.7	6.2	0.023
24	Me	Me	0.003	>25	>25	>25	0.043
25	-CH_2CH_2-		0.0007	29.7	12.2	8.5	0.012
26	-$CH_2CH_2CH_2$-		0.004	>25	>25	>25	0.236
33			0.0004	>25	2.7	3.2	0.001
34			0.001	>25	4.1	13.1	0.016
35			0.003	>25	22.2	29.7	0.248
36			0.0008	>25	4.2	3.6	0.005
37			0.0005	>25	1.9	0.7	0.002
38			0.002	>25	4.7	6.4	0.017
39			0.011	>25	2.6	13.3	1.340
40			0.001	>25	4.6	5.7	0.371
41			0.004	>25	15.8	38.0	0.816
42			0.026	>25	>25	>25	0.391
43			0.002	>25	17.0	7.1	0.029
44			0.010	>25	33.6	39.4	0.044
45			0.007	>25	16.2	63.3	0.572
46			0.006	>25	24.9	22.9	0.091

[a]IC_{50} values are the mean of at least two independent experiments. The errors of the IC_{50} values are within a factor of 1.6. [b]A20/DO10.11 antigen-presentation assay.

Table 3. hCatS and mCatS Activity of Cyclopentane 21 and Proline Derivatives 75−79 Are Very Similar

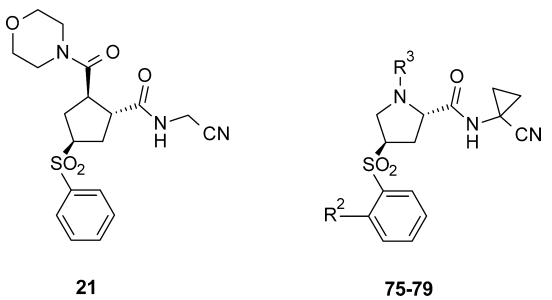

			IC_{50} (μM)[a]					
compd	R^2	R^3	hCatS enzyme	mCatS enzyme	hCatK enzyme	hCatL enzyme	hCatB enzyme	A20 cell-based[b]
21			0.0007	0.001	15.5	11.7	6.2	0.023
75	CF_3	H	0.002	0.006	>25	>25	>25	0.058
76	H	Ph−C(O)	0.013	0.029	>25	>25	>25	0.217
77	Cl	Ph−C(O)	0.0008	0.001	>25	6.8	35.2	0.015
78	Cl	Cyclohexyl-C(O)	0.0003	0.0002	>25	8.3	14.9	0.002
79	Cl	Me-C(O)	0.001	0.002	>25	29.7	47.6	0.019

[a]IC_{50} values are the mean of at least two independent experiments. The errors of the IC_{50} values are within a factor of 1.6. [b]A20/DO10.11 antigen-presentation assay.

administration, and circulating IL-2 levels were determined 4 h postdosing as a marker of T-cell activation. Proline derivative **75** did not reduce ovalbumin-mediated IL-2 production at a dose as high as 50 mg/kg despite the high plasma levels of 2053 ng/mL achieved. The lack of activity was hypothesized to be related to the very low volume of distribution of the compound (Vd_{ss} = 0.13 L/kg), in the range of plasma to extracellular volume. In contrast, acetamide **79** (Vd_{ss} of 0.50 L/kg) showed a dose-

dx.doi.org/10.1021/jm401528k | J. Med. Chem. XXXX, XXX, XXX−XXX

Table 4. PK Properties of 21, 75, and 79 in Mice[a]

	AUC/dose (1 mg) (ng h/mL)		$t_{1/2}$ (h)				
compd	iv[b]	po[c]	iv[b]	po[c]	Vd_{ss} (L/kg)	Cl (mL/min/kg)	F (%)
21	427	77	0.3	0.9	0.50	39	18
75	10 400	7200	1.1	0.9	0.13	1.6	69
79	581	309	0.3	0.5	0.50	29	53

[a]All values given are the mean of two experiments. [b]For iv, compound (2 mg) was dissolved in aqueous NaCl/*N*-methyl-2-pyridone. [c]For po, compound (9 mg) was used as a microsuspension in gelatin/aqueous NaCl.

dependent reduction in IL-2 (Figure 5), with an ED_{50} of 5 mg/kg. Free exposure levels at ED_{50} were estimated to be in the range of the IC_{50} determined in the cell-based assay.

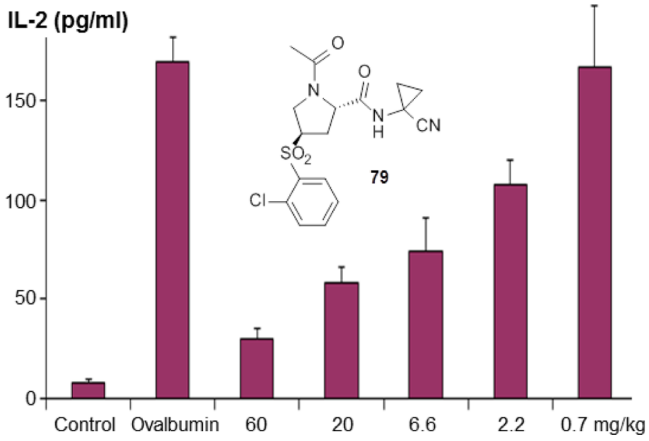

Figure 5. Dose-dependent reduction of IL-2 in DO10.11 mice by proline-derivative **79** 4 h after oral postdose (n = 8; mean reduction as compared to ovalbumin challenge). All compound treatments except the 0.7 mg/kg group are significantly different than the ovalbumin challenge group ($p < 0.05$, ANOVA followed by multiple Dunnett test).

In the light of the observed in vivo PD effect demonstrated, the prototype proline derivative **79** certainly looks promising as a starting point but needs further optimization. Properties to be improved include plasma stability, metabolic stability, the short half-life, and the low volume of distribution. Optimization of the proline series leading eventually to a clinical candidate will be the subject of a future communication.

SUMMARY AND CONCLUSIONS

Structure-based design of weakly active dual CatS/K inhibitor **5** (IC_{50} = 0.830/0.855 μM) lead to potent and selective cyclopentane derivative **22** (IC_{50} = 0.0005/>25 μM, CatS/K) by utilizing specific interactions in the S2 pocket of CatS. The S3 pocket turned out to be tolerable for R^3 modifications, allowing the tuning of physicochemical properties. Scaffold hopping from cyclopentane **22** to analogous pyrrolidine derivative **57** reduced the cellular activity significantly (IC_{50} = 0.003 and 0.208 uM, respectively) but was regained with proline derivative **78** (IC_{50} = 0.002 uM). The X-ray structure of three compounds (**21**, **56**, and **57**) bound to mCatS revealed specific favorable and unfavorable interactions: (1) the high potency of cyclopentane derivative **21** can be explained by a favorable network of edge-to-face interactions of three aromatic units in the S2 pocket, (2) conformational strain was significantly reduced in the more potent cyclopentane-sulfone scaffold **21** compared to pyrrolidine-sulfonamide **56**, and (3) sigma-hole interactions between a chlorine and the sulfur atom of M194 in combination with vdW interactions of chlorine with the hydrogens of the C-epsilon of M194 and the movement of Y334 that yielded a face-to-face interaction boosted the potency in **22** and **57** compared to their des-chloro counterparts **21** and **56**. Proline derivative **79** turned out to be active in vivo, reducing IL-2 in a transgenic DO10.11 mouse model sensitized to ovalbumin with an ED_{50} of 5 mg/kg. Liabilities of the proline series could be overcome in lead optimization, delivering a clinical candidate that will be discussed in a future paper.

EXPERIMENTAL SECTION

General. All solvents and reagents were obtained from commercial sources and were used as received. All reactions were followed by TLC (TLC plates F254, Merck) or LCMS (liquid chromatography–mass spectrometry) analysis. Silica gel chromatography was either performed using cartridges packed with silica gel (ISOLUTE Columns, TELOS Flash Columns) on ISCO Combi Flash Companion or on glass columns on silica gel 60 (32-60 mesh, 60 Å). ^{1}H NMR spectra were obtained on Bruker Avance 300 or 400 MHz spectrometer with chemical shifts (δ in ppm) reported relative to tetramethylsilane or the residual solvent peak as the internal reference (i.e., $CDCl_3$ = 7.26 ppm, DMSO-d_6 = 2.50 ppm). ^{1}H resonances are reported to the nearest 0.01 ppm. NMR abbreviations are as follows: s, singlet; d, doublet; t, triplet; q, quadruplet; quint, quintuplet; sext, sextuplet; m, multiplet; br, broadened. Coupling constants (J) are reported to the nearest 0.1 Hz. Purity was analyzed by reverse-phase HPLC performed on Finnigan LTQ (Thermo Fisher Scientific) and Agilent RRLC 1200 equipment. Column: Agilent XDB C15, 30 mm × 4.6 mm, 3.5 μm. Analytical conditions: gradient used, 5 to 95% acetonitrile in water containing 0.1% trifluoroacetic acid in 3 min. Flow: 4.5 mL/min. UV detector: DAD 190–400 nm. Sample solvent: in water/acetonitrile (8:2). The UV detection was an averaged signal from wavelengths of 190–400 nm. Mass spectra were recorded on an SSQ 7000 (Finnigan-MAT) spectrometer for electron impact ionization. LC-HRMS spectra were recorded with an Agilent LC system consisting of an Agilent 1290 high-pressure system, a CTC PAL auto sampler, and an Agilent 6520 QTOF. The separation was achieved on a Zorbax Eclipse Plus C18 1,7 μm 2.1*30 mm column at 55 °C; eluent A = 0.01% formic acid in water, B = 0.01% formic acid in acetonitrile/2-propanol (8:2); flow, 1 mL/min. Gradient: 0 min 5% of B, 0.3 min 5% of B, 4.5 min 99% of B, 5 min 99% of B. The injection volume was 2 μL. All assay compounds had a purity of >95% according to HPLC. LC–MS (ESI, positive or negative ion) data were recorded on Waters UPLC-MS systems equipped with Waters Acquity, a CTC PAL auto sampler, and a Waters SQD single quadrupole mass spectrometer using ES ionization modes (positive and/or negative). The separation was achieved on a Zorbax Eclipse Plus C18 1,7 μm 2.1*30 mm column at 50 °C; A = 0.01% formic acid in water, B = acetonitrile at flow 1; gradient: 0 min 3% B, 0.2 min 3% B, 2 min 97% B, 1.7 min 97% B, 2.0 min 97% B. The injection volume was 2 μL. MS (ESI, positive or negative ion): FIA (flow injection analysis)-MS were recorded on a AppliedBiosystem API150 mass spectrometer. Sample introduction was made with a CTC PAL auto sampler and a Shimadzu LC-10ADVP pump. The samples were directly flushed to the ESI source of the mass spectrometer with a flow of 50 μL/min of a mixture of acetonitrile and 10 mM ammonium acetate (1:1) without a column. The injection volume was 2 μL.

dx.doi.org/10.1021/jm401528k | J. Med. Chem. XXXX, XXX, XXX–XXX

General Procedure A for the Amide Formation from an Acid and an Amine using EDCI/HOBt. To a solution of the acid (10.0 mmol) in tetrahydrofuran (25 mL) were subsequently added the amine (15 mmol), triethylamine (70 mmol), 1-hydroxybenzotriazole hydrate (20 mmol), and 1-(3-dimethylaminopropyl)-3-ethylcarbodiimide hydrochloride (EDCI, 20 mmol), and stirring was continued at 22 °C overnight. The mixture was evaporated, the residue partitioned between ethyl acetate and 1N aqueous HCl, and the organic layer was washed with saturated aqueous Na_2CO_3, dried, and evaporated to give the crude amide.

General Procedure B for the Amide Formation from an Acid and an Amine using *i*-Butyl Chloroformate. A solution of the acid (0.12 mmol) and 4-methyl-morpholine (0.3 mmol) in tetrahydrofuran (2 mL) was cooled to −16 °C and treated with *i*-butyl chloroformate (20 mg, 0.14 mmol), and stirring was continued for 30 min. The amine (17 mg, 0.14 mmol) was added, the mixture was allowed to warm to 22 °C, and stirring was continued overnight. The mixture was partitioned between aqueous saturated $NaHCO_3$, the organic layer was washed with hydrochloric acid (1 N), dried, and evaporated, and the residue was purified by preparative HPLC on a RP-18 column using a gradient of a mixture of acetonitrile and water to give the amide.

General Procedure C for the Hydrolysis of an Ester to the Carboxylic Acid. To a solution of the ester (1.35 mmol) in THF (10 mL) were added a solution of LiOH (3.0 mmol) in water (3 mL) and methanol (3 mL), and stirring was continued at 22 °C until the conversion was completed. The mixture was evaporated, and the residue was partitioned between ethyl acetate and hydrochloric acid (0.1 N). The organic layer was dried and evaporated to give the crude acid.

General Procedure D for the Synthesis of a Mesylates from an Alcohol. To a solution of the alcohol (10.0 mmol) in dichloromethane (110 mL) were added at 5 °C triethylamine (40.0 mmol) and methanesulfonyl chloride (40.0 mmol), and stirring was continued at 5 °C until the conversion was completed. The mixture was partitioned between aqueous HCl (1 N) and dichloromethane, and the organic layer was washed with aqueous Na_2CO_3 solution (half saturated), dried, and evaporated to give the crude mesylate.

General Procedure E for the Synthesis of a Thioether from a Mesylate and a Thiol. To a solution of the thiol (0.75 mmol) in THF (4 mL) was added NaH (55% in oil, 0.75 mmol) at 22 °C, and the mixture was stirred until gas evolution ceased. A solution of the mesylate (175 mg, 0.50 mmol) in THF (1 mL) was added, and the mixture was heated at 50 °C until the conversion was completed. The mixture was partitioned between aqueous Na_2CO_3 and EtOAc, and the organic layer was dried and evaporated to give the crude thioether.

General Procedure F for the Oxidation of a Thioether to the Sulfone. To a solution of the thioether (0.25 mmol) in dichloromethane (2.5 mL) was added a solution of *m*-chloroperbenzoic acid (70%, 1 mmol) in dichloromethane (2.5 mL), and stirring was continued at 22 °C until the conversion was completed. The mixture was vigorously shaken with aqueous $NaHSO_3$ (20%), the organic layer was washed with saturated aqueous Na_2CO_3 and water, and the organic layer was dried and evaporated to give the crude sulfone.

General Procedure G for the Formation of a Sulfonamide from an Amine. To a solutiuon of the amine (12 mmol) and diisopropylethylamine (36 mmol) in acetonitrile (30 mL) was added the sulfonyl chloride (14 mmol) at 22 °C, and stirring was continued at 22 °C overnight. The mixture was partitioned between an aqueous Na_2CO_3 solution and EtOAc, and the organic layer was washed with hydrochloric acid (0.1 N), dried, and evaporated to give the crude sulfonamide.

General Procedure H for the Deprotection of the Boc Group to the Amine. A solution of the Boc-protected amine (2.5 mmol) in dichloromethane (15 mL) was treated with trifluoracetic acid (25 mmol), and stirring was continued at 22 °C until the conversion was completed. The solution was evaporated to give the crude amine as the salt with trifluoro-acetic acid, which was processed in the next step without further purification.

*(1R,2R)-4-Oxo-cyclopentane-1,2-dicarboxylic Acid Monoethyl Ester (**2**).*[11] Racemic *trans*-4-oxo-cyclopentane-1,2-dicarboxylic acid diethyl ester (**1**)[15] (60.44 g, 264.8 mmol) was emulsified under vigorous stirring in MES buffer (1.16 L) containing 2-(*N*-morpholino)-ethanesulfonic acid (1.13 g, 5 mM) and magnesium diacetate tetrahydrate (12.44 g, 50 mM). After pH adjustment to 6.2 using a NaOH solution, CALB L (1.94 mL, a liquid formulation of lipase from *Candida antarctica* B, Novozymes, Denmark) was added at 22 °C, and the was pH kept constant at 6.2 under vigorous stirring by automated addition (pH-stat) of a 1.0 M NaOH solution. After consumption of 118.3 mL (ca. 45% conversion after 42 h reaction time; enantiomeric excess of formed acid still >95%), dichloromethane (1.0 L) was added, and the aqueous phase was washed with dichloromethane (3 × 1.5 L), the pH was set to 3.0 using phosphoric acid (85%), and the aqueous phase was extracted with ethyl acetate (4 × 1.0 L). The combined ethyl acetate phases were dried over sodium sulfate and filtered, and the filtrate was evaporated and dried under high vacuum overnight to give title compound **2** (24.40 g, 46%) as white crystals. Chemical purity: 99.8% (GC, analyzed as the methylester; same conditions as the ee determination). Optical purity: 95.2% ee (GC, analyzed as the methylester on a BGB-176 column, 30 m × 0.25 mm; H_2; 100 to 200 °C with 2 °C/min). $[\alpha]_{589}$ (20 °C) −101.2° (*c* 1.0; EtOH). ^{1}H NMR (400 MHz, $CDCl_3$) δ 4.14−4.30 (m, 2H), 3.33−3.50 (m, 2H), 2.65−2.78 (m, 2H), 2.48−2.61 (m, 2H), 1.29 (t, J = 7.1 Hz, 3H). MS (ESI, negative ion): 199.1 $[M - H]^-$.

*(1R,2R)-2-(Morpholine-4-carbonyl)-4-oxo-cyclopentanecarboxylic Acid Ethyl Ester (**3**).*[11] The amide formation of (1*R*,2*R*)-4-oxo-cyclopentane-1,2-dicarboxylic acid monoethyl ester (**2**) (5.00 g, 25 mmol) and morpholine according to general procedure A gave crude title compound **3** (5.95 g, 88%) as a pale-yellow oil, which was used in the next step without further purification. MS: 270.2 $(M + H)^+$.

*(1R,2R,4R)-4-Hydroxy-2-(morpholine-4-carbonyl)-cyclopentanecarboxylic Acid Ethyl Ester (**6**).*[11] A mixture of (1*R*,2*R*)-2-(morpholine-4-carbonyl)-4-oxo-cyclopentanecarboxylic acid ethyl ester (**3**) (7.77 g, 28.85 mmol) in 148 mL of aqueous buffer (289 mg (10 mM) 2-(*N*-morpholino)ethanesulfonic acid, 15.5 g (0.5 M) D-glucose monohydrate [2.7 equ.], and 65 mg (2 mM) magnesium chloride hexahydrate) was adjusted to pH 6.5. Under stirring, the reduction was started at 22 °C by the addition of the cofactor NADP (779 mg [0.03 equ.]), the cofactor regeneration enzyme glucose dehydrogenase (77 mg GDH 102 [Codexis]), and the ketoreductase (387 mg KRED-NADP-131 [Codexis]). During the 21h reaction, the pH was maintained at 6.5 by the addition of 31.9 mL of 1 M NaOH (pH-stat). Under stirring, the mixture was adjusted to pH 2.8, saturated with 43.6 g of sodium chloride, and stirred for at least 10 min after the addition of 17 g of filter aid (Dicalite) and 300 mL of ethyl acetate. Subsequently, the filter aid was removed, and the filtrate was adjusted to pH 7.0 prior to extraction. After phase separation, the aqueous phase was extracted three times with 300 mL of ethyl acetate. The combined organic phases were dried with sodium sulfate and filtered, the filtrate was evaporated, and the residue was dried overnight under high vacuum to give title compound **6** (7.1 g, 91%) as a pale-yellow oil. Chiral GC: ee 95.2% [BGB-176, 30m; H_2; 2 °C/min, 150 to 220 °C]. ^{1}H NMR (400 MHz, DMSO-d_6) δ 4.72 (d, J = 3.9 Hz, 1H), 4.10−4.18 (m, 1H), 4.04 (q, J = 7.1 Hz, 2H), 3.41−3.61 (m, 10H), 3.17 (td, J = 8.1, 9.9 Hz, 1H), 2.19 (ddd, J = 5.4, 9.9, 13.1 Hz, 1H), 1.78−1.88 (m, 1H), 1.57−1.74 (m, 2H), 1.16 (t, J = 7.1 Hz, 3H). MS: 272.1 $[M + H]^+$.

*(1R,2R,4R)-4-Methanesulfonyloxy-2-(morpholine-4-carbonyl)-cyclopentanecarboxylic Acid Ethyl Ester (**7**).*[11] (1*R*,2*R*,4*R*)-4-Hydroxy-2-(morpholine-4-carbonyl)-cyclopentanecarboxylic acid ethyl ester (**6**) (2.20 g, 10.0 mmol) was converted according to procedure D to the crude mesylate, which was purified by flash chromatography using EtOAc to give title compound **7** (2.60 g, 91%) as a pale-yellow oil. ^{1}H NMR (300 MHz, $CDCl_3$) δ 5.24 (tt, J = 2.5, 5.2 Hz, 1H), 4.16 (q, J = 7.1 Hz, 2H), 3.51−3.75 (m, 9H), 3.34−3.46 (m, 1H), 3.01 (s, 3H), 2.45−2.59 (m, 1H), 2.25−2.41 (m, 2H), 2.08−2.22 (m, 1H), 1.27 (t, J = 7.1 Hz, 3H). MS: 350.1 $[M + H]^+$.

*(1R,2R,4S)-2-(Morpholine-4-carbonyl)-4-phenylsulfanyl-cyclopentanecarboxylic Acid Ethyl Ester (**9**).*[11] (1*R*,2*R*,4*R*)-4-Methanesulfonyloxy-2-(morpholine-4-carbonyl)-cyclopentanecarboxylic acid ethyl ester (**7**) (0.91 g, 2.6 mmol) and thiophenol were converted according to general procedure E to the crude thioether, which was purified by flash chromatography using *n*-hepane/EtOAc (3:2) to give title compound **9** (0.47 g, 50%) as a pale-yellow oil. ^{1}H NMR (300 MHz, $CDCl_3$) δ 7.19−7.41 (m, 5H), 4.12 (q, J = 7.1 Hz, 2H), 3.26−3.74 (m,

dx.doi.org/10.1021/jm401528k | J. Med. Chem. XXXX, XXX, XXX−XXX

11H), 2.23−2.47 (m, 2H), 2.09−2.22 (m, 1H), 1.82 (td, J = 9.7, 13.0 Hz, 1H), 1.24 (t, J = 7.1 Hz, 3H). MS: 364.5 $[M + H]^+$.

*(1R,2R,4S)-4-(2-Chloro-phenylsulfanyl)-2-(morpholine-4-carbonyl)-cyclopentanecarboxylic Acid Ethyl Ester (**10**).*[11] (1*R*,2*R*,4*R*)-4-Methanesulfonyloxy-2-(morpholine-4-carbonyl)-cyclopentanecarboxylic acid ethyl ester (**7**) (175 mg, 0.5 mmol) and 2-chlorothiophenol were converted according to general procedure E to the crude thioether, which was purified by flash chromatography using *n*-hepane/EtOAc (3:2) to give title compound **10** (113 mg, 57%) as a colorless oil. ^{1}H NMR (300 MHz, $CDCl_3$) δ 7.34−7.42 (m, 2H), 7.12−7.25 (m, 2H), 4.13 (q, J = 7.1 Hz, 2H), 3.32−3.79 (m, 11H), 2.29−2.50 (m, 2H), 2.09−2.23 (m, 1H), 1.87 (td, J = 9.6, 13.1 Hz, 1H), 1.25 (t, J = 7.2 Hz, 3H). MS: 398.1 $[M + H]^+$.

*(1R,2R,4S)-2-(Morpholine-4-carbonyl)-4-(2-trifluoromethyl-phenylsulfanyl)-cyclopentanecarboxylic Acid Ethyl Ester (**11**).*[11] (1*R*,2*R*,4*R*)-4-Methanesulfonyloxy-2-(morpholine-4-carbonyl)-cyclopentanecarboxylic acid ethyl ester (**7**) (300 mg, 0.86 mmol) and 2-trifluoromethylthiophenol were converted according to general procedure E to the crude thioether, which was purified by flash chromatography using cyclohexane/EtOAc (1:2) to give title compound **10** (304 mg, 82%) as a colorless oil. ^{1}H NMR (300 MHz, $CDCl_3$) δ 7.67 (d, J = 7.8 Hz, 1H), 7.55 (d, J = 7.8 Hz, 1H), 7.47 (t, J = 7.8 Hz, 1H), 7.32 (t, J = 7.8 Hz, 1H), 4.12 (q, J = 7.1 Hz, 2H), 3.66 (d, J = 3.2 Hz, 11H), 2.27−2.47 (m, 2H), 2.10−2.24 (m, 1H), 1.88 (td, J = 10.0, 13.0 Hz, 1H), 1.24 (t, J = 7.1 Hz, 3H). MS: 432.3 $[M + H]^+$.

*(1R,2R,4S)-4-Benzenesulfonyl-2-(morpholine-4-carbonyl)-cyclopentanecarboxylic Acid Ethyl Ester (**13**).*[11] (1*R*,2*R*,4*S*)-2-(Morpholine-4-carbonyl)-4-phenylsulfanyl-cyclopentanecarboxylic acid ethyl ester (**9**) (783 mg, 2.15 mmol) was converted according to general procedure F to the crude sulfone, which was purified by flash chromatography using *n*-heptane/EtOAc (1:3) to give title compound **13** (857 mg, quantitative) as a colorless oil. ^{1}H NMR (300 MHz, $CDCl_3$) δ 7.85−7.96 (m, 2H), 7.63−7.72 (m, 1H), 7.53−7.62 (m, 2H), 4.10 (d, J = 7.1 Hz, 2H), 3.25- 3.70 (m, 11H), 2.48−2.63 (m, 1H), 2.06−2.36 (m, 3H), 1.23 (t, J = 7.1 Hz, 3H). MS: 396.1 $[M + H]^+$.

*(1R,2R,4S)-4-(2-Chloro-benzenesulfonyl)-2-(morpholine-4-carbonyl)-cyclopentanecarboxylic Acid Ethyl Ester (**14**).*[11] (1*R*,2*R*,4*S*)-4-(2-Chloro-phenylsulfanyl)-2-(morpholine-4-carbonyl)-cyclopentanecarboxylic acid ethyl ester (**10**) (100 mg, 0.25 mmol) was converted according to general procedure F to the crude sulfone, which was purified by flash chromatography using *n*-heptane/EtOAc (1:3) to give title compound **14** (92 mg, 85%) as a colorless oil. ^{1}H NMR (300 MHz, $CDCl_3$) δ 8.13−8.18 (m, 1H), 7.43−7.63 (m, 3H), 4.18−4.33 (m, 1H), 4.12 (q, J = 7.1 Hz, 2H), 3.28−3.74 (m, 10H), 2.50−2.65 (m, 1H), 2.02−2.38 (m, 3H), 1.24 (t, J = 7.1 Hz, 3H). MS: 430.5 $[M + H]^+$.

*(1R,2R,4S)-2-(Morpholine-4-carbonyl)-4-(2-trifluoromethyl-benzenesulfonyl)-cyclopentanecarboxylic Acid Ethyl Ester (**15**).*[11] (1*R*,2*R*,4*S*)-2-(Morpholine-4-carbonyl)-4-(2-trifluoromethyl-phenylsulfanyl)-cyclopentanecarboxylic acid ethyl ester (**11**) (304 mg, 0.70 mmol) was converted according to general procedure F to the crude sulfone, which was purified by flash chromatography using EtOAc to give title compound **15** (324 mg, 99%) as a colorless oil. ^{1}H NMR (300 MHz, $CDCl_3$) δ 8.24−8.32 (m, 1H), 7.88−7.98 (m, 1H), 7.73−7.83 (m, 2H), 4.12 (q, J = 7.2 Hz, 2H), 3.84−4.01 (m, 1H), 3.25−3.76 (m, 10H), 2.62 (ddd, J = 7.9, 9.8, 13.8 Hz, 1H), 2.27−2.43 (m, 1H), 2.05−2.22 (m, 2H), 1.23 (t, J = 7.2 Hz, 3H). MS: 464.1 $[M + H]^+$.

*(1R,2R,4S)-4-Benzenesulfonyl-2-(morpholine-4-carbonyl)-cyclopentanecarboxylic Acid (**17**).*[11] (1*R*,2*R*,4*S*)-4-Benzenesulfonyl-2-(morpholine-4-carbonyl)-cyclopentanecarboxylic acid ethyl ester (**13**) (853 mg, 2.16 mmol) was converted according to general procedure C to crude acid **17** (780 mg, 98%), which was processed without further purification. MS (ESI, negative ion): 366.3 $[M - H]^-$.

*(1R,2R,4S)-4-(2-Chloro-benzenesulfonyl)-2-(morpholine-4-carbonyl)-cyclopentanecarboxylic Acid (**18**).*[11] (1*R*,2*R*,4*S*)-4-(2-Chloro-benzenesulfonyl)-2-(morpholine-4-carbonyl)-cyclopentanecarboxylic acid ethyl ester (**14**) (80 mg, 0.19 mmol) was converted according to general procedure C to crude acid **18** (93 mg, quantitative), which was processed without further purification. MS: 402.1 $[M + H]^+$.

*(1R,2R,4S)-2-(Morpholine-4-carbonyl)-4-(2-trifluoromethyl-benzenesulfonyl)-cyclopentanecarboxylic Acid (**19**).*[11] (1*R*,2*R*,4*S*)-2-(Morpholine-4-carbonyl)-4-(2-trifluoromethyl-benzenesulfonyl)-cyclopentanecarboxylic acid ethyl ester (**15**) (324 mg, 0.70 mmol) was converted according to general procedure C to crude acid **19** (286 mg, 94%), which was processed without further purification. MS (ESI, negative ion): 434.4 $[M - H]^-$.

*(1R,2R,4R)-4-Benzenesulfonyl-2-(morpholine-4-carbonyl)-cyclopentanecarboxylic Acid Cyanomethyl-amide (**21**).*[11] (1*R*,2*R*,4*S*)-4-Benzenesulfonyl-2-(morpholine-4-carbonyl)-cyclopentanecarboxylic acid (**17**) (369 mg, 0.91 mmol) dissolved in DMF (8 mL) was reacted according to general procedure A with aminoacetonitrile hydrochloride to give the crude amide, which was purified by flash chromatography using EtOAc to give title compound **21** (156 mg, 42%) as a white solid. ^{1}H NMR (300 MHz, $CDCl_3$) δ 7.85−7.96 (m, 2H), 7.64−7.73 (m, 1H), 7.54−7.63 (m, 2H), 7.07 (t, J = 6.0 Hz, 1H), 4.17 (dd, J = 6.0, 16.0 Hz, 1H), 4.03 (dd, J = 6.0, 16.0 Hz, 1H), 3.34−3.81 (m, 10H), 2.98−3.21 (m, 1H), 2.20−2.49 (m, 4H). LC-HRMS: m/z $(M + H)^+$ calcd for $C_{19}H_{23}N_3O_5S$, 406.1431; found, 406.1436.

*(1R,2R,4R)-4-(2-Chloro-benzenesulfonyl)-2-(morpholine-4-carbonyl)-cyclopentanecarboxylic Acid Cyanomethyl-amide (**22**).*[11] (1*R*,2*R*,4*S*)-4-(2-Chloro-benzenesulfonyl)-2-(morpholine-4-carbonyl)-cyclopentanecarboxylic acid (**18**) (45 mg, 0.09 mmol) dissolved in THF (0.7 mL) and DMF (0.7 mL) was reacted according to general procedure A with aminoacetonitrile hydrochloride to give the crude amide, which was purified by flash chromatography using dichloromethane/MeOH (60:1) to give title compound **22** (8 mg, 20%) as a white solid. ^{1}H NMR (300 MHz, CDCl3) δ 8.09−8.20 (m, 1H), 7.43−7.64 (m, 3H), 7.20 (t, J = 6.0 Hz, 1H), 4.27−4.42 (m, 1H), 4.17 (dd, J = 6.0, 17.4 Hz, 1H), 4.05 (dd, J = 6.0, 17.4 Hz, 1H), 3.10−3.74 (m, 10H), 2.21−2.45 (m, 4H). LC-HRMS: m/z $(M + H)^+$ calcd for $C_{19}H_{22}ClN_3O_5S$, 440.1041; found, 440.1052.

*(1R,2R,4R)-2-(Morpholine-4-carbonyl)-4-(2-trifluoromethyl-benzenesulfonyl)-cyclopentanecarboxylic Acid Cyanomethyl-amide (**23**).*[11] (1*R*,2*R*,4*S*)-2-(Morpholine-4-carbonyl)-4-(2-trifluoromethyl-benzenesulfonyl)-cyclopentanecarboxylic acid (**19**) (80 mg, 0.18 mmol) dissolved in DMF (3 mL) was reacted according to general procedure A with aminoacetonitrile hydrochloride to give the crude amide, which was purified by flash chromatography using EtOAc to give title compound **23** (77 mg, 89%) as a white foam. ^{1}H NMR (300 MHz, $CDCl_3$) δ 8.24−8.33 (m, 1H), 7.91−8.00 (m, 1H), 7.75−7.85 (m, 2H), 6.97 (t, J = 6.0 Hz, 1H), 4.17 (dd, J = 6.0, 17.4 Hz, 1H), 4.05 (dd, J = 6.0, 17.4 Hz, 1H), 3.39−3.75 (m, 10H), 3.02−3.17 (m, 1H), 2.27−2.43 (m, 4H). LC-HRMS: m/z $(M + H)^+$ calcd for $C_{20}H_{22}F_3N_3O_5S$, 474.1305; found, 474.1317.

*(2S,4S)-Methyl-4-methanesulfonyloxy-N-Boc-pyrrolidine-2-carboxylate (**60**).*[30] (2*S*,4*S*)-Methyl-4-hydroxy-*N*-Boc-pyrrolidine-2-carboxylate (**59**) (1.00 g, 4.1 mmol) was converted according to general procedure D to the crude mesylate, which was purified by flash chromatography using cyclohexane/EtOAc (1:2) to give title compound **60** (1.33 g, quantitative) as a pale-yellow oil. ^{1}H NMR (300 MHz, $CDCl_3$) δ 5.18−5.29 (m, 1H), 4.35−4.59 (m, 1H), 3.72−3.85 (m, 2H), 3.76 (s, 3H), 3.01 (s, 3H), 2.43−2.59 (m, 2H), 1.48 and 1.43 (s each, 9H). MS: 324.4 $[M + H]^+$.

*(2S,4R)-Methyl-4-(2-chloro-phenylsulfanyl)-N-Boc-pyrrolidine-2-carboxylate (**62**).*[12] (2*S*,4*S*)-Methyl-4-methanesulfonyloxy-*N*-Boc-pyrrolidine-2-carboxylate (**60**) (1.00 g, 3.1 mmol) and 2-chlorothiophenol were converted according to general procedure E to the crude thioether, which was purified by flash chromatography using EtOAc to give title compound **62** (0.644 g, 70%) as a white solid. ^{1}H NMR (300 MHz, $CDCl_3$) δ 7.36−7.46 (m, 2H), 7.26 (s, 2H), 4.35−4.55 (m, 1H), 3.84−4.02 (m, 2H), 3.74 (s, 3H), 3.34−3.55 (m, 1H), 2.18−2.43 (m, 2H), 1.45 and 1.42 (s each, 9H). MS: 372.1 $[M + H]^+$.

*(2S,4R)-Methyl-4-(2-chloro-benzenesulfonyl)-N-Boc-pyrrolidine-2-carboxylate (**65**).*[12] (2*S*,4*R*)-Methyl-4-(2-chloro-phenylsulfanyl)-*N*-Boc-pyrrolidine-2-carboxylate (**62**) (0.64 g, 1.7 mmol) was converted according to general procedure F to the crude sulfone, which was purified by flash chromatography using cyclohexane/EtOAc (1:1) to give title compound **65** (0.60 g, 86%) as a colorless oil. ^{1}H NMR (300 MHz, $CDCl_3$) δ 8.05−8.18 (m, 1H), 7.55−7.67 (m, 2H), 7.45−7.54 (m, 1H), 4.32−4.62 (m, 2H), 3.57−4.02 (m, 5H), 2.58−2.98 (m, 1H), 2.09−2.41 (m, 1H), 1.45 and 1.40 (s each, 9H). MS: 404.5 $[M + H]^+$.

*(2S,4R)-4-(2-Chloro-benzenesulfonyl)-N-Boc-pyrrolidine-2-carboxylic Acid (**68**).*[12] (2*S*,4*R*)-Methyl-4-(2-chloro-benzenesulfonyl)-*N*-

dx.doi.org/10.1021/jm401528k | J. Med. Chem. XXXX, XXX, XXX−XXX

Boc-pyrrolidine-2-carboxylate (**65**) (3.60 g, 8.9 mmol) was hydrolyzed according to general procedure C to crude acid **68** (3.47 g, quantitative), which was used in the next step without purification. MS (ESI, negative ion): 388.3 $[M - H]^-$.

*(2S,4R)-4-(2-Chloro-benzenesulfonyl)-2-(1-cyano-cyclopropylcarbamoyl)-N-Boc-pyrrolidine (**71**).*[12] (2*S*,4*R*)-4-(2-Chloro-benzenesulfonyl)-*N*-Boc-pyrrolidine-2-carboxylic acid (**68**) (5.0 g, 12.8 mmol) and 1-amino-cyclopropanecarbonitril hydrochloride were converted according to general procedure B to the crude amide, which was purified by flash chromatography using *n*-heptane/EtOAc (gradient from 1:0 to 1:1) to give title compound **71** (4.70 g, 87%) as a colorless foam. ^{1}H NMR (300 MHz, $CDCl_3$) δ 8.08−8.14 (m, 1H), 7.89 (br. s., 1H), 7.57−7.67 (m, 2H), 7.46−7.54 (m, 1H), 4.36−4.54 (m, 2H), 4.00 (dd, J = 6.3, 12.1 Hz, 1H), 3.61 (dd, J = 7.9, 11.5 Hz, 1H), 2.57−2.74 (m, 1H), 2.26−2.44 (m, 1H), 1.44−1.54 (m, 11H), 1.15−1.23 (m, 2H). MS: 454.4 $[M + H]^+$.

*(2S,4R)-4-(2-Chloro-benzenesulfonyl)-2-(1-cyano-cyclopropylcarbamoyl)-pyrrolidine; Salt with Hydrochloric Acid (**74**).*[12] A solution of (2*S*,4*R*)-4-(2-chloro-benzenesulfonyl)-2-(1-cyano-cyclopropylcarbamoyl)-*N*-Boc-pyrrolidine (**71**) (408 mg, 0.9 mmol) in HCl/1,4-dioxane (2 M, 4 mL) was stirred at 22 °C overnight, the suspension was filtered, and the residue washed with diethyl ether and dried to give amine hydrochloride **74** (280 mg, 80%) as a white solid. MS: 354.1 $[M + H]^+$.

*(2S,4R)-1-Acetyl-4-(2-chloro-benzenesulfonyl)-pyrrolidine-2-carboxylic acid (1-Cyano-cyclopropyl)-amide (**79**).*[12] To a mixture of (2*S*,4*R*)-4-(2-chloro-benzenesulfonyl)-2-(1-cyano-cyclopropylcarbamoyl)-pyrrolidine (salt with hydrochloric acid) (**74**) (293 mg, 0.75 mmol) in acetonitrile (15 mL) were added diisopropylethylamine (582 mg, 4.5 mmol) and acetic anhydride (368 mg, 3.6 mmol), and stirring was continued at 22 °C for 3 h. The mixture was partitioned between saturated aqueous Na_2CO_3 and EtOAc, and the organic layer was washed with 1 N aqueous HCl, dried, and evaporated to give the crude amide, which was purified by flash chromatography using *n*-heptane/EtOAc (gradient, 2:3 to 1:5) to give title compound **79** (167 mg, 56%) as a colorless foam. ^{1}H NMR (300 MHz, CDCl3) δ 8.10−8.15 (m, 1H), 7.97 (s, 1H), 7.60−7.68 (m, 2H), 7.47−7.55 (m, 1H), 4.55−4.75 (m, 2H), 4.05−4.17 (m, 1H), 3.77−3.86 (m, 1H), 2.62−2.75 (m, 1H), 2.25−2.35 (m, 1H), 2.16 (s, 3H), 1.45−1.55 (m, 2H), 1.15−1.25 (m, 2H). LC-HRMS: m/z $(M + H)^+$ calcd for $C_{17}H_{18}ClN_3O_4S$, 396.0779; found, 396.0779.

Cathepsin S, K, L, and B Enzyme Inhibition Assay. Enzyme activity was measured by observing the increase in fluorescence intensity caused by cleavage of a peptide substrate containing a fluorophore whose emission is quenched in the intact peptide. Assay buffer: 100 mM potassium phosphate, pH 6.5, EDTA-Na 5 mM, Triton X-100 0.001%, and DTT 5 mM. Enzymes (all at 1 nM): human and mouse cathepsin S and mouse CatK, CatL, and CatB. Substrate (20 μM): Z-Val-Val-Arg-AMC except for CatK, which uses Z-Leu-Arg-AMC (both from Bachem). Final volume: 100 μL. Excitation 360 nm, emission 465 nm. Enzyme was added to the substance dilutions in 96-well microtiter plates, and the reaction was started with substrate. Fluorescence emission was measured over 20 min, during which time a linear increase was observed in the absence of inhibitor. IC_{50} values were calculated by standard methods.

Cell-Based Assay. A20 cells (ATCC, no. 30-2001) were plated at 3 × 10^5 cells/ml in 100 μL/well of a U-bottom 96-well plate. Compounds were added, and cells were incubated for 1 h before the addition of ovalbumin to a final concentration of 5 mg/mL (Sigma Aldrich). After 16 h, the cells were washed three times with PBS, and 2 × 10^5 DO10.10 T-cell hybridoma cells/ml were added. After 24 h, IL-2 production was measured by Luminex single-bead analysis using two anti-IL-2 antibodies (BD, cat. nos. 554424 and 554426).

LogD Determination. LogD determination was carried out as described.[31]

Cell Permeability Determination. Cell permeability was determined as described.[29]

Protein Crystallography. *Cloning and Protein Expression.* The mouse Cathepsin S (mCatS) gene without a secretion signal (coding for amino acids A22−I340 with L97S compared to UniProt O70370) was amplified from lung cDNA by PCR. NdeI and NotI restriction enzyme sites at the 5′ and 3′ ends, respectively, were used to clone the gene into a pET24 vector. No tag was added to the N- or C-terminus. The protein was produced in *Escherichia coli* strain BL21 (DE3)RIL at 37 °C in LB medium by induction with IPTG (isopropyl thio-β-D-galactoside).

Isolation and Solubilization of Inclusion Bodies (IBs). Cell pellets (20g) were resuspended in 50 mM Tris-HCl (120 mL), pH 8.0, supplemented with 2 mM ethylendiaminetetraacetic acid (EDTA), 5% saccharose, 30 mg/mL DNase I, and 30 mg/mL RNase I (fresh). After cell disruption and centrifugation, IBs were washed with 50 mM Tris-HCl, pH 8.0, containing 2 mM EDTA and 0.1% Triton X-100 and centrifuged again. The washing procedure was repeated twice with a second buffer (50 mM Tris-HCl, pH 8.0, and 1 M urea). The final pellet was solubilized in 50 mM Tris-HCl (15 mL), pH 8.0, 5 mM EDTA, 6 M guanidinium hydrochloride, 150 mM NaCl, and 10 mM dithiothreitol (DTT) and centrifuged at 4 °C, and the protein concentration of mCatS was determined via HPLC.

Folding and Reoxidation of Mouse Procathepsin S. The IB solution was diluted to a protein concentration of 4.4 mg/mL and subsequently diluted 1:100 using a sample pump with a flow rate of 0.6 mL/min in 50 mM Tris-HCl buffer, pH 8.5, 500 mM L-arginine, 0.01% BRIJ 35, 100 mM NaCl, 80 mL catalase (1 mg/mL), 10 mM glutathione (GSH), and 1 mM glutathione disulfide (GSSG) at 4 °C. The mixture was stirred for 48 h at 4 °C, filtered, concentrated, and dialyzed at 4 °C against 25 mM sodium phosphate buffer, pH 7.0, and 500 mM NaCl overnight.

Purification of mCatS. The protein solution was adjusted to a final concentration of 1500 mM $(NH_4)_2SO_4$ and centrifuged, the supernatant was loaded on a HIC Toyopearl-Butyl650 column equilibrated with 10 mM Tris-HCl, pH 8.0, 1 M NaCl, 1.5 M $(NH_4)_2SO_4$, and 0.01% NaN_3, and the column was eluted with a linear gradient to 10 mM Tris-HCl, pH 8.0, and 0.01% NaN_3. The pooled fractions were concentrated and loaded on a Superdex 75 (XK26/100) column equilibrated with 20 mM sodium acetate at pH 4.5, 300 mM NaCl, 5 mM DTT, 2.5 mM EDTA, 0.01% NaN_3, and 0.01% BRIJ35. Autoactivation was performed during size-exclusion chromatography, and fractions containing mCatS were pooled and concentrated around 20-fold with a 10 kDa cutoff ultrafiltration membrane.

Active-Site Cysteine Oxidation. The integrity of the active-site cysteine was analyzed by titration with the covalent, irreversible inhibitor *N*-morpholinourea-leucine-homophenylalanine-vinylsulfone-phenyl (LHVS). Initially, oxidation of this cysteine appeared to be a problem, but this was overcome by the inclusion of catalase in the refolding step. By taking care to degas buffers and to work and store protein under argon, the amount of mCatS with an oxidized active-site cysteine could be reduced to around 30%.

Removal of Oxidized CatS by (S−S) Covalent Chromatography. Concentrated and activated mCatS was loaded onto a Fast Desalting column HR10/10 (GE Heathcare) equilibrated in 100 mM sodium acetate buffer, pH 4.0, and 1 mM EDTA. The DTT-free mCatS fraction was subsequently applied to a Thiopropyl Sepharose 6B column (2.6 × 5 cm, GE Healthcare). The part of the protein sample with an oxidized active-site cysteine was collected in the column flow-through. Active mCatS was eluted in 25 mM sodium acetate buffer, pH 4.5, 300 mM NaCl, 10% glycerin, 0.01% BRIJ35, and 2.5 mM EDTA containing 10 mM DTT. The mCatS pool was concentrated and passed over a Fast desalting HR10/10 equilibrated in 100 mM sodium acetate, pH 4.5, containing 5 mM DTT and 5 mM EDTA. Aliquots showing over 97% active, nonoxidized mCatS were stored under argon in sealed tubes at −80 °C.

*Cocrystallization of mCatS in Complex with **21**, **56**, **57**, and **75**.* Protein at a concentration of 2 μM in 100 mM sodium acetate pH 4.5, 5 mM DTT, 5 mM EDTA, and 0.01% NaN_3 was incubated with ligand in a 10-fold molar excess overnight at 4 °C under argon. Prior to crystallization experiments, the protein was concentrated to 21−36 mg/mL and centrifuged at 20 000*g*. The crystallization droplets for **21** and **75** were set up at 22 °C by mixing 0.25 μL of protein solution with 0.25 μL of reservoir solution (Index Screen, Hampton Research) in microbatch experiments under Al's oil (Hampton Research). For the cocrystallization of **56** and **57**, vapor-diffusion experiments in sitting-drop set ups were used. For compound **21**, crystals were obtained out of 2 M $(NH_4)_2SO_4$ (pH 5.5) as precipitant. Complexes with compounds

dx.doi.org/10.1021/jm401528k | J. Med. Chem. XXXX, XXX, XXX−XXX

56 and **57** crystallized out of 25% PEG 3350 (pH 7.5 and 6.5, respectively), and the complex with compound **75** crystallized out of 3 M sodium citrate (pH 3.5). Before data collection, crystals were transferred to crystallization buffer supplemented with 20% glycerol or 20% ethylene glycol and flash-frozen in liquid N_2. Data collection and evaluation and structure determination were performed as described with minor modifications.[28]

Pharmacokinetic Experiments in Mice and Plasma Stability Studies. *Animals and Housing Conditions.* Animal experiments were conducted during the light phase and under ad libitum conditions. Animal housing and experimental procedures were in line with ethical and legal guidelines and were authorized by local veterinary authorities.

In Vivo Experiment. C57Bl/6 male mice (8 week old; 24−29 g; Charles River Laboratories, Germany GmbH) received doses of the test compound by po gavage (9 mg/kg as an aqueous microsuspension in gelatin/NaCl (7.5%/0.62%)) and iv bolus (2 mg/kg in aqueous NaCl/30% 1-methyl-2-pyrrolidone). The nominal concentration of the compound in the formulation was adjusted to reach a 4 mL/kg oral dosage or a 2 mL/kg iv bolus. Terminal blood samples (500 mL, $n = 2$ per time point) were taken at different time points postdosing by decapitation and collected in precooled EDTA-coated tubes. The samples were kept on ice and immediately centrifuged at 4 °C to obtain plasma. Samples were stored at −20 °C until analysis.

Plasma in Vitro stability. Heparinized pooled human or NMRI mouse plasma samples were spiked with 1000 ng/mL of the compound of interest. Incubations were performed in a thermostatted orbital shaker at 37 °C. Aliquots ($n = 3$ per time point) were taken after 2 min, 1 h, and 4 h of incubation and immediately processed for analysis.

LC−MS/MS Compound Analysis. Quantification of compound levels in plasma was accomplished by means of LC−MS/MS analysis. Plasma (50 mL) was precipitated in three volumes of acetonitrile containing d_6-midazolam (0.2 mg/mL) as an internal standard, mixed, and centrifuged (10 min, 4 °C, 5850*g*). The supernatant was diluted 1:1 with water and injected onto a Phenomenex Gemini C18 3 μm 2.0·30 mm column operating with mobile phases A (0.2% formic acid in water containing 5% acetonitrile) and B (acetonitrile) at 0.3 mL/min flow. The outlet of the column was coupled to an API3000 mass spectrometer (AB Sciex, Brugg, Switzerland) with TurboIonSpray source. Detection was carried out using multiple reactions monitoring mode with positive ion detection to follow compound-specific transitions.

IL-2 Reduction in DO10.11 Transgenic Mice. Animals and Housing Conditions. Animals were maintained in a 12 h:12 h light/dark cycle, with lights on starting at 6 a.m., and experiments were conducted during the light phase. Animal housing and experimental procedures were in line with ethical and legal guidelines and were authorized by local veterinary authorities.

Experiment. DO10.11 BALBc mice were used to test the role of CatS in antigen presentation. These mice express a transgenic TCR recognizing an ovalbumin peptide. Challenge of the mice with 1.0 mg iv low-endotoxin ovalbumin results in rapid production of interleukin 2 by T cells. Increased levels of IL-2 were detected at the 4 h time point in plasma using Luminex bead technology and two anti-IL-2 antibodies (BD nos. 554424 and 554426).

■ ASSOCIATED CONTENT

Ⓢ Supporting Information

Preparation details and analytical data for compounds **5**, **20**, **24**−**26**, **33**−**46**, **56**−**58**, and **74**−**78**; and distribution of torsion angles observed for alkyl-sulfones and alkyl-sulfonamides in the small-molecule crystal structures database. This material is available free of charge via the Internet at http://pubs.acs.org.

Accession Codes

Crystal structure coordinates and structure factors have been deposited in the PDB under accession numbers 4BSQ (**21**), 4MZO (**56**), 4MZS (**57**), and 4BS5 (**75**).

■ AUTHOR INFORMATION

Corresponding Authors

*Phone: +41 61 688 72 64. E-mail: hans.hilpert@roche.com (H.H.).

*Phone: +41 61 688 68 93. E-mail: wolfgang.haap@roche.com (W.H.).

Notes

The authors declare no competing financial interest.

■ ACKNOWLEDGMENTS

We thank P. Bourdeaux, M. Marti, and S. Thomi for synthesis, P. Hartman, A. Araujo Del Rosario, and R. Ecabert for screening, J. Schneider for NMR, and C. Bartelmus for mass spectroscopy support.

■ ABBREVIATIONS USED

AMC, 7-amino-4-methyl-coumarin BOC, *t*-butoxycarbonyl; DAST, diethylaminosulfur trifluoride; DMF, *N*,*N*-dimethylformamide, DMSO, dimethyl sulfoxide; DTT, dithiothreitol; EDCI, 1-ethyl-3-(3-dimethylaminopropyl)carbodiimid; EtOAc, ethyl acetate; EtOH, ethanol; HOBt, 1-hydroxybenzotriazol; MeOH, methanol; NADP, nicotinamide adenine dinucleotide phosphate; TEA, triethylamine; TFA, trifluoro-acetic acid; THF, tetrahydrofuran; Z, benzyloxycarbonyl

■ REFERENCES

(1) Turk, B.; Turk, V.; Turk, D. Structural and functional aspects of papain-like cysteine proteinases and their protein inhibitors. *Biol. Chem.* **1997**, *378*, 141−150.

(2) Podolin, P. L.; Bolognese, B. J.; Carpenter, D. C.; Davis, T. G.; Johanson, R. A.; Fox, J. H.; Long, E.,, III; Dong, X.; Marquis, R. W.; LoCastro, S. M.; Terfloth, G. J.; Kurali, E.; Peterson, J. J.; Smith, B. R.; McQueney, M. S.; Yamashita, D. S.; Capper-Spudich, E. A. Inhibition of invariant chain processing, antigen-induced proliferative responses, and the development of collagen-induced arthritis and experimental autoimmune encephalomyelitis by a small molecule cysteine protease inhibitor. *J. Immunol.* **2008**, *180*, 7989−8003.

(3) Biroc, S. L.; Gay, S.; Hummel, K.; Magill, C.; Palmer, J. T.; Spencer, D. R.; Sa, S.; Klaus, J. L.; Michel, B. A.; Rasnick, D.; Gay, R. E. Cysteine protease activity is up-regulated in inflamed ankle joints of rats with adjuvant-induced arthritis and decreases with in vivo administration of a vinyl sulfone cysteine protease inhibitor. *Arthritis Rheum.* **2001**, *44*, 703−711.

(4) Nakagawa, T. Y.; Brissette, W. H.; Lira, P. D.; Griffiths, R. J.; Petrushova, N.; Stock, J.; McNeish, J. D.; Eastman, S. E.; Howard, E. D.; Clarke, S. R. M.; Rosloniec, E. F.; Elliott, E. A.; Rudensky, A. Y. Impaired invariant chain degradation and antigen presentation and diminished collagen-induced arthritis in cathepsin S null mice. *Immunity* **1999**, *10*, 207−217.

(5) Shi, G.-P.; Villadangos, J. A.; Dranoff, G.; Small, C.; Gu, L.; Haley, K. J.; Riese, R.; Ploegh, H. L.; Chapman, H. A. Cathepsin S required for normal MHC class II peptide loading and germinal center development. *Immunity* **1999**, *10*, 197−206.

(6) Lee-Dutra, A.; Wiener, D. K.; Sun, S. Cathepsin S inhibitors: 2004−2010. *Expert Opin. Ther. Pat.* **2011**, *21*, 311−337.

(7) Gauthier, J. Y.; Black, W. C.; Courchesne, I.; Cromlish, W.; Desmarais, S.; Houle, R.; Lamontagne, S.; Li, C. S.; Masse, F.; McKay, D. J.; Ouellet, M.; Robichaud, J.; Truchon, J.-F.; Truong, V.-L.; Wang, Q.; Percival, M. D. The identification of potent, selective, and bioavailable cathepsin S inhibitors. *Bioorg. Med. Chem. Lett.* **2007**, *17*, 4929−4933.

(8) Bekkali, Y.; Thomson, D. S.; Betageri, R.; Emmanuel, M. J.; Hao, M.-H.; Hickey, E.; Liu, W.; Patel, U.; Ward, Y. D.; Young, E. R. R.; Nelson, R.; Kukulka, A.; Brown, M. L.; Crane, K.; White, D.; Freeman, D. M.; Labadia, M. E.; Wildeson, J.; Spero, D. M. Identification of a novel class of succinyl-nitrile-based cathepsin S inhibitors. *Bioorg. Med. Chem. Lett.* **2007**, *17*, 2465−2469.

(9) Moss, N.; Xiong, Z.; Burke, M.; Cogan, D.; Gao, D. A.; Haverty, K.; Heim-Riether, A.; Hickey, E. R.; Nagaraja, R.; Netherton, M.; O'Shea, K.; Ramsden, P.; Schwartz, R.; Shih, D.-T.; Ward, Y.; Young, E.; Zhang, Q. Exploration of cathepsin S inhibitors characterized by a triazole P1-P2 amide replacement. *Bioorg. Med. Chem. Lett.* **2012**, *22*, 7189−7193.
(10) Gabriel, T.; Pech, M.; Rodriguez, S. R. M. β-Amino acid nitrile derivatives useful for the treatment of diseases which are associated with cysteine proteases. Patent WO2001096285A1, 2001.
(11) Banner, D.; Ceccarelli, S. M.; Grether, U.; Haap, W.; Hilpert, H.; Kuehne, H.; Mauser, H.; Plancher, J.-M.; Sanchez, R. A. Novel cyclopentane derivatives as cysteine protease cathepsin inhibitors and their preparation and use in the treatment of diseases. Patent WO2010142650A1, 2010.
(12) Sanchez, R. A.; Banner, D.; Ceccarelli, S. M.; Grether, U.; Haap, W.; Hartman, P.; Hartmann, G.; Hilpert, H.; Kuehne, H.; Mauser, H.; Plancher, J.-M. Preparation of proline dipeptidyl nitrile derivatives as cathepsin, particularly cathepsin S and L, inhibitors. Patent US20100267722A1, 2010.
(13) Kim, M.; Jeon, J.; Song, J.; Suh, K. H.; Kim, Y. H.; Min, K. H.; Lee, K.-O. Synthesis of proline analogues as potent and selective cathepsin S inhibitors. *Bioorg. Med. Chem. Lett.* **2013**, *23*, 3140−3144.
(14) Banner, D.; Haap, W.; Kuhn, B.; Luebbers, T.; Peters, J.-U.; Schulz-Gasch, T. Preparation of substituted 4-(phenylsulfonyl)-pyrrolidine-2-carboxamide derivatives as cathepsin inhibitors. Patent WO2013076063A1, 2013.
(15) Mittendorf, J.; Benet-Buchholz, J.; Fey, P.; Mohrs, K.-H. Efficient asymmetric synthesis of β-amino acid BAY 10-8888/PLD-118, a novel antifungal for the treatment of yeast infections. *Synthesis* **2003**, 136−140.
(16) Kataoka, M.; Kita, K.; Wada, M.; Yasohara, Y.; Hasegawa, J.; Shimizu, S. Novel bioreduction system for the production of chiral alcohols. *Appl. Microbiol. Biotechnol.* **2003**, *62*, 437−445.
(17) Kosjek, B.; Nti-Gyabaah, J.; Telari, K.; Dunne, L.; Moore, J. C. Preparative asymmetric synthesis of 4,4-dimethoxytetrahydro-2H-pyran-3-ol with a ketone reductase and in situ cofactor recycling using glucose dehydrogenase. *Org. Process Res. Dev.* **2008**, *12*, 584−588.
(18) Rodriguez, S. R. M.; Wirz, B.; Iding, H. Chemoenzymatic preparation of non-racemic N-Boc-pyrrolidine-3,4-dicarboxylic acid 3-ethyl esters and their 4-hydroxymethyl derivatives. *Tetrahedron: Asymmetry* **2003**, *14*, 1547−1551.
(19) McGrath, M. E.; Palmer, J. T.; Bromme, D.; Somoza, J. R. Crystal structure of human cathepsin S. *Protein Sci.* **1998**, *7*, 1294−1302.
(20) Oballa, R. M.; Truchon, J.-F.; Bayly, C. I.; Chauret, N.; Day, S.; Crane, S.; Berthelette, C. A generally applicable method for assessing the electrophilicity and reactivity of diverse nitrile-containing compounds. *Bioorg. Med. Chem. Lett.* **2007**, *17*, 998−1002.
(21) *The PyMOL Molecular Graphics System*, version 1.5; Schrödinger, LLC; http://www.pymol.org.
(22) McGrath, M. E.; Klaus, J. L.; Barnes, M. G.; Broemme, D. Crystal structure of human cathepsin K complexed with a potent inhibitor. *Nat. Struct. Biol.* **1997**, *4*, 105−109.
(23) Brameld, K. A.; Kuhn, B.; Reuter, D. C.; Stahl, M. Small molecule conformational preferences derived from crystal structure data. A medicinal chemistry focused analysis. *J. Chem. Inf. Model.* **2008**, *48*, 1−24.
(24) Menziani, M. C.; Cocchi, M.; De, B. P. G. Electronic and electrostatic aspects of carbonic anhydrase inhibition by sulfonamides. *J. Mol. Struct.: THEOCHEM* **1992**, *88*, 217−229.
(25) Allen, F. H. The Cambridge Structural Database: A quarter of a million crystal structures and rising. *Acta Crystallogr., Sect. B* **2002**, *58*, 380−388.
(26) Cambridge Crystallographic Data Centre Home Page. http://www.ccdc.cam.ac.uk.
(27) Wilcken, R.; Zimmermann, M. O.; Lange, A.; Zahn, S.; Kirchner, B.; Boeckler, F. M. Addressing methionine in molecular design through directed sulfur-halogen bonds. *J. Chem. Theory Comput.* **2011**, *7*, 2307−2315.
(28) Hardegger, L. A.; Kuhn, B.; Spinnler, B.; Anselm, L.; Ecabert, R.; Stihle, M.; Gsell, B.; Thoma, R.; Diez, J.; Benz, J.; Plancher, J.-M.; Hartmann, G.; Isshiki, Y.; Morikami, K.; Shimma, N.; Haap, W.; Banner, D. W.; Diederich, F. Halogen bonding at the active sites of human cathepsin L and MEK1 kinase: Efficient interactions in different environments. *ChemMedChem* **2011**, *6*, 2048−2054.
(29) Kansy, M.; Senner, F.; Gubernator, K. Physicochemical high throughput screening: Parallel artificial membrane permeation assay in the description of passive absorption processes. *J. Med. Chem.* **1998**, *41*, 1007−1010.
(30) Tsunoda, H.; Fukumura, K. Process for producing ester or alcohol. Patent WO2007148435A1, 2007.
(31) Hilpert, H.; Guba, W.; Woltering, T. J.; Wostl, W.; Pinard, E.; Mauser, H.; Mayweg, A. V.; Rogers-Evans, M.; Humm, R.; Krummenacher, D.; Muser, T.; Schnider, C.; Jacobsen, H.; Ozmen, L.; Bergadano, A.; Banner, D. W.; Hochstrasser, R.; Kuglstatter, A.; David-Pierson, P.; Fischer, H.; Polara, A.; Narquizian, R. β-Secretase (BACE1) inhibitors with high in vivo efficacy suitable for clinical evaluation in Alzheimer's disease. *J. Med. Chem.* **2013**, *56*, 3980−3995.